Intense electromagnetic radiation from relativistic particles

V. A. Bazylev and N. K. Zhevago

I. V. Kurchatov Institute of Atomic Energy, Moscow
Usp. Fiz. Nauk **137**, 605–662 (August 1982)

Several mechanisms for emission of electromagnetic radiation by relativistic electrons in various media which are of interest for generating intense ultraviolet, x-ray, and γ radiation are examined. Theoretical and experimental results on ultraviolet and x-ray Cherenkov radiation, quasi-Cherenkov radiation in artificial periodic structures, radiation from crystals which results from the diffraction of virtual photons, and radiation accompanying channeling are discussed.

PACS numbers: 61.80.Mk

CONTENTS

INTRODUCTION

This review has primarily two purposes. First, we wish to call attention to the fact that there are several mechanisms by which relativistic electrons can emit electromagnetic radiation in various media which are of interest for developing sources of intense ultraviolet, x, or γ radiation for applications. Second, we wish to review the relatively recent theoretical and experimental results on several new phenomena in the electromagnetic emission by relativistic electrons—results which have not yet been covered in a review.

Sources of intense radiation ranging from the ultraviolet region to hard x rays are of course widely used in a variety of scientific and technological fields. By "intense" source we mean a radiation source which has a high spectral-angular emission intensity, i.e., which emits a rather large number of photons in a given energy interval in a given solid-angle interval per unit time. Ultraviolet and x radiation at wavelengths from 1000 Å down to 1 Å are used in such traditional fields as the absorption spectroscopy of solids and gases[1-4] and the x-ray structural analysis of ordered systems.[4,5] On the other hand, there are several new fields of application of such radiation, e.g., in the lithographic manufacture of electronic microcircuits[6,7] and in molecular biology.[4,8] Harder radiation, with wavelengths $\lesssim$0.1 Å, is used in nuclear spectroscopy, in particular, Mossbauer spectroscopy,[9] to study photonuclear reactions,[10] and to produce intense neutron fluxes from these reactions.[11] There has also been a recent discussion of the possibility of pumping nuclear and electronic levels by x radiation with the goal of developing x-ray and γ-ray lasers.[12]

Radiation at wavelengths greater than 600 Å can be produced in electric discharges in discharge tubes filled with hydrogen, inert gases, or the vapor of some other material.[1-4] Harder monochromatic radiation, with wavelengths between 0.1 and 10 Å, arises in x-ray tubes. This radiation occurs during the filling of those vacancies which appear in the electron shells of atoms of the anode material as a result of bombardment of the anode by electrons.

The usual source of hard x and γ radiation is the bremsstrahlung of relativistic electrons. Where highly monochromatic radiation is required, use is made of the γ emission during inflight positron annihilation[10,13] and in (n,γ) reactions[9] or the γ rays produced in the scattering of a laser beam by relativistic electrons.[4,14]

These radiation sources are the most common sources at present. There has also been a recent discussion of the possible widespread use of the magnetobremsstrahlung x radiation which is produced in syn-

 0038-5670/82/080565-31$01.80

chrotrons and storage rings[4,5,15] and also in various spatially periodic magnetic structures (undulators and wigglers).[16-20] There are yet several other emission mechanisms of interest for applications: ultraviolet and x-ray Cherenkov radiation, the transition (quasi-Cherenkov) radiation in crystals, the emission which accompanies the channeling of electrons in crystals, and several others. In certain frequency intervals, the intensities of the corresponding sources (per electron) may exceed by several orders of magnitude the intensities of not only the conventional sources but also synchrotron radiation. At the moment, most of these interesting emission mechanisms have received extremely little experimental study or none at all. It is thus our hope that this review will also contribute to design of experiments to test the theoretical predictions.

1. CHERENKOV RADIATION

a) Radiation in an absorbing medium

Cherenkov radiation from a charged particle occurs at the frequency ω when the velocity (v) of the particle in a homogeneous nonabsorbing medium exceeds the phase velocity of light,[21] $c/\sqrt{\varepsilon'(\omega)}$. The condition $v>c/\sqrt{\varepsilon'}$ can usually be satisfied in the optical frequency range for a broad range of media, and most of the theoretical and experimental research which has been carried out has accordingly been devoted to the properties of Cherenkov radiation in the optical frequency range, where photon-absorption effects can usually be ignored.[21-26]

Cherenkov radiation can also occur, however, at shorter wavelengths, in the ultraviolet[27,28] and x-ray[29-31] ranges. Here the effect of the absorbing properties of the medium on the shaping of the spectral and angular distributions of the radiation becomes extremely important.

The need to consider the effect of absorption on the Cherenkov radiation follows from simple physical considerations based on the concept of a radiation coherence length. The coherence length was introduced by Ter-Mikaelyan[32] in a theoretical analysis of bremsstrahlung in single crystals. This general characteristic of radiation by fast particles in a medium has since then been used effectively to analyze radiation mechanisms and hadron processes.[33]

The emission does not occur instantaneously. It is necessary at the very least that the particle and the radiation wave move apart by a distance of the order of the wavelength. Let us assume that an electron, moving at a constant velocity, radiates a Cherenkov-radiation wave at the characteristic angle $\theta_0=\arccos(1/v\sqrt{\varepsilon'})$. While the wave lags behind the electron by a distance equal to the wavelength, λ, along the direction in which the electron is moving, the electron has time to travel a distance equal to the coherence length, l_{coh}. The wave velocity in the medium is $c/\sqrt{\varepsilon'}$. The coherence length for Cherenkov radiation is thus found from

$$(v-c(\varepsilon')^{-1/2}\cos\theta_0)\frac{l_{\mathrm{coh}}}{v}=\lambda. \tag{1.1}$$

Under the condition $\varepsilon'-1\ll 1$, for ultrarelativistic velocities, $v\approx c[1-(1/2\gamma^2)]$, and small angles, $\theta_0\ll 1$, we find from this equation[23,24]

$$l_{\mathrm{coh}}=\frac{\lambda}{\varepsilon'(\omega)-1-\gamma^{-2}} \tag{1.2}$$

($\gamma=E/mc^2$, E is the energy of the particle, and m is its mass).

The photon absorption length in the medium, $l_c(\omega)$ is determined by $l_c=\lambda/\varepsilon''$, where $\varepsilon''(\omega)$ is the imaginary part of the dielectric permittivity. If the coherence length l_{coh} exceeds the absorption length l_c, it is clear that the classical Tamm-Frank results[21] for the spectral distribution of the Cherenkov radiation will have to be substantially modified. The governing parameter for this effect is the ratio

$$\frac{l_{\mathrm{coh}}}{l_c}=\frac{\varepsilon''(\omega)}{\varepsilon'(\omega)-1-\gamma^{-2}}.$$

Another factor which must in general be taken into account if the Cherenkov radiation occurs at small angles, $\theta_0\ll 1$, is multiple scattering of electrons in the medium.[34-36]

A measure of the multiple-scattering effect can also be extracted from the simple calculations above. For this purpose we replace the particle velocity v in (1.1) by the projection of this velocity onto the original direction of the particle, $v\cos\theta_s$, where $\cos\theta_s\approx 1-(\theta_s^2/2)$, and $\theta_s^2=ql_{\mathrm{coh}}$ is the mean square angle of the multiple scattering over the coherence length. As a result we find that we may ignore the effect of multiple scattering on the radiation as long as the square of the multiple-scattering angle over the coherence length is less than the square of the Cherenkov-radiation angle, i.e.,

$$\frac{q\lambda}{(\varepsilon'-1-\gamma^{-2})^2}\ll 1. \tag{1.3}$$

In the opposite case, the deviation of the electron from a rectilinear trajectory during the radiation must be taken into account. This has been done[34-36] for an infinite medium; we will not reproduce the lengthy results here.

As a rule, however, multiple scattering has a negligible effect on the radiation spectrum in comparison with absorption, because absorption comes into play over far shorter distances: $l_c(\omega)\ll\sqrt{c/q\omega}$.

There is an important aspect of the radiation by relativistic particles in an absorbing medium. If the coherence length becomes comparable to the photon absorption length, only the total energy loss of the particle can be discussed meaningfully: There is no unambiguous way to distinguish the radiation loss from the overall energy loss in this case.[36] The reason is that the photons are absorbed before they have time to form, so that the criterion for distinguishing "emitted" photons from virtual photons breaks down. In particular, in an infinite absorbing medium, at frequencies such that the imaginary part of the dielectric permittivity, $\varepsilon''(\omega)$, is determined by the photoelectric effect or by atomic excitation, the Cherenkov radiation is seen only as an addition to the ionization energy loss of relativistic electrons.

Another possibility for observing Cherenkov radiation in the presence of absorption is to detect the electromagnetic energy flux beyond a slab of the absorbing medium.

The spectral-angular electromagnetic energy density emitted in a slab of thickness T by a charge moving along a rectilinear path at a relativistic velocity $v \approx c[1-(\gamma^{-2}/2)]$ is (see Ref. 37, for example)

$$\frac{d^2W}{d\omega\, d\Omega} = \frac{e^2}{\pi^2 c}\theta^2 |A(\omega,\theta)|^2,$$

$$A(\omega,\theta) = \left\{1-\exp\left[-\frac{i\omega T}{2c}(1-\varepsilon+\gamma^{-2}+\theta^2)\right]\right\} \times \left[\frac{1}{1-\varepsilon+\gamma^{-2}+\theta^2} - \frac{1}{\gamma^{-2}+\theta^2}\right]; \tag{1.4}$$

$\theta \ll 1$ is the polar angle of the emission, $d\Omega \approx \theta d\theta d\varphi$ is the element of solid angle, and $\varepsilon(\omega) = \varepsilon'(\omega) + i\varepsilon''(\omega)$.

If the slab thickness is much greater than the photon absorption length in the medium $[T \gg l_c(\omega)]$, the exponential function can be ignored in the expression for $A(\omega,\theta)$. In this case, after integrating (1.4) over angles, we find the spectral distribution of the radiation from a semi-infinite slab to be

$$\frac{dW}{d\omega} = \frac{e^2}{2\pi c}\left\{\left[\left(1+\frac{2\gamma^{-2}(1-\varepsilon')}{(1-\varepsilon')^2+(\varepsilon'')^2}\right)\ln\frac{(1-\varepsilon'+\gamma^{-2})^2+(\varepsilon'')^2}{\gamma^{-4}} - 2\right] - \frac{2}{\varepsilon''}\left[1-\varepsilon'+\gamma^{-2}\frac{(1-\varepsilon')^2-(\varepsilon'')^2}{(1-\varepsilon')^2+(\varepsilon'')^2}\right]\left(\frac{\pi}{2} - \operatorname{arctg}\frac{1-\varepsilon'+\gamma^{-2}}{\varepsilon''}\right)\right\}. \tag{1.5}$$

At frequencies at which the ratio of the absorption length to the coherence length of the emission is small, $\varepsilon' - 1 - \gamma^{-2} \ll \varepsilon''$, the first term in braces is predominant in (1.5). This term represents the spectral density of the transition radiation. Even if the condition $(v\sqrt{\varepsilon'}/c) - 1 \approx (\varepsilon' - 1 - \gamma^{-2})/2 > 0$ can be satisfied, the Cherenkov radiation is greatly suppressed by the absorption of the medium in this case.

In the opposite case of weak absorption, expression (1.5) becomes

$$\frac{dW}{d\omega} = \frac{e^2\omega}{c^2}(\varepsilon'-1-\gamma^{-2})\,\eta(\varepsilon'-1-\gamma^{-2})\,l_c(\omega) + \frac{e^2}{2\pi c}\left[\left(1-\frac{2}{\gamma^2(1-\varepsilon')}\right)\ln\frac{(1-\varepsilon'+\gamma^{-2})^2}{\gamma^{-4}} - 2\right], \tag{1.6}$$

where $\eta(z)$ is the Heaviside unit step function. In the absence of Cherenkov radiation ($\varepsilon' - 1 - \gamma^{-2} < 0$) the second term can be interpreted as the spectral energy density of the transition radiation. In particular, at frequencies for which the "plasma" expression, $\varepsilon'(\omega) = 1 - (\omega_p^2/\omega^2)$, holds the second term is equal to the result derived by Garibyan[38] for the spectral density of x-ray transition radiation. When Cherenkov radiation can occur, however, the second term in (1.6) can take on negative values near the threshold for Cherenkov radiation ($\gamma^{-2} \approx \varepsilon' - 1$). In this case the second term must be reinterpreted as an effect of the boundary of the medium on the Cherenkov radiation. The first term in (1.6) is the spectral density of the Cherenkov radiation with this boundary effect ignored. It can be derived from the results of Tamm and Frank[21] for the spectral energy density of Cherenkov radiation in a nonabsorbing infinite medium by considering only a trivial absorption of the radiation in the medium itself.

We will see that even in a transparent medium there are conditions under which the Cherenkov radiation and the transition radiation of a relativistic particle cannot be discussed separately. This is particularly true when there is absorption, and it is not possible to distinguish either the intensity of the transition radiation or that of the Cherenkov radiation in (1.5) in the common meaning of these terms. All that can be said is that the Cherenkov radiation continuously transforms into transition radiation with increasing value of the parameter l_{coh}/l_c. The situation here is completely analogous to the case of an infinite absorbing medium, in which the Cherenkov radiation cannot be unambiguously distinguished from the overall energy loss under the condition[36] $l_{coh}/l_c \sim 1$.

Although multiple scattering does not affect the spectral distribution of the radiation, because of the stronger effect of the photon absorption, it can still cause a spreading of the angular distribution in thick targets. Expression (1.4) thus gives a correct description of the spectral-angular distribution of the radiation if the target is not too thick: $q_T \ll \varepsilon' - 1 - \gamma^{-2}$.

It is this case with which we will be dealing below. In this case the angular distribution of the Cherenkov radiation near the direction $\theta_0 = \sqrt{\varepsilon' - 1 - \gamma^{-2}}$ is determined by diffraction over the absorption length according to (1.4):

$$S_{Cer} \equiv \left.\frac{d^2W}{\hbar\, d\omega\, d\Omega}\right|_{\theta=\theta_0} \approx 7.4\cdot 10^{-4}\frac{\varepsilon'-1-\gamma^{-2}}{(\varepsilon'')^2}. \tag{1.7}$$

With a source of electrons with energy E and a gaseous medium in which Cherenkov radiation can occur, we can arrange conditions, by adjusting the gas pressure, such that the given energy is only a few times the threshold energy $E_{th} = (\varepsilon' - 1)^{-1/2} mc^2$. By comparing the spectral density of the Cherenkov radiation, (1.7), with the corresponding expression for synchrotron radiation, we find

$$\frac{S_{Cer}}{S_{sy}} \sim \frac{(\varepsilon'-1)^2}{(\varepsilon'')^2}, \tag{1.8}$$

$$\frac{dW_{Cer}}{d\omega}\left(\frac{dW_{sy}}{d\omega}\right)^{-1} \sim \frac{(\varepsilon'-1)}{\varepsilon''}. \tag{1.9}$$

The spectral-angular density and the spectral density of the Cherenkov radiation per particle are thus substantially higher than the corresponding values for the synchrotron radiation, since the condition $\varepsilon' - 1 \gg \varepsilon''$ must hold at Cherenkov-radiation frequencies.

In terms of the spectral-angular density, Cherenkov radiation can be comparable to the radiation from an undulator[20] with $N = (\varepsilon' - 1)/\varepsilon''$ periods. Admittedly, the undulator has the advantage that, when installed in a straight section of a storage ring, it has essentially no effect on the dynamics of the stored electron beam. At the same time, a target of thickness ~1 μm can attenuate a beam rather quickly. As will be shown below, however, the advantage of Cherenkov radiation over undulator radiation is that x rays can be generated by electrons with energies of only a few MeV by the Cherenkov mechanism, in comparison with the hundreds of MeV which would be required in undulators.[16-20]

b) Ultraviolet Cherenkov radiation

There are several materials in which the binding energy of the valence electrons is quite high, and the real

TABLE I. Materials in which ultraviolet Cherenkov radiation can occur.[27] (λ_c is the critical wavelength; the data for the gases correspond to 0°C and 1 atm)

Material	λ_c, Å	Refractive index at λ=2500 A
Helium	584	1.000036
Neon	736	1.000069
Argon	1048	1.0003
LiF	1050	1.418
CaF_2	1350	1.4673
Sapphire	1425	1.845
High-purity fused silicon	1650	1.5074

part of the dielectric permittivity, $\varepsilon'(\omega)$, is greater than unity at ultraviolet frequencies (Table I). Foremost in this group are the inert gases.

Figure 1, from Ref. 27, shows the wavelength dependence of the dielectric permittivity of helium at standard pressure and standard temperature. The real part of the dielectric permittivity, $\varepsilon'(\omega)$, is greater than unity over a broad frequency range. The extent to which it exceeds unity is $\sim 10^{-4}$, and the corresponding threshold for Cherenkov radiation is $E_{th} \approx 50$ MeV. It follows from Refs. 27 and 28 that at wavelengths $\lambda \geqslant 620$ Å the ratio $(\varepsilon' - 1)/\varepsilon'' \sim 10^2$ is much larger than unity, so that there is the possibility of intense Cherenkov radiation for particles with energies $E > E_{th}$.

Figure 2 shows theoretical and experimental values of the spectral photon flux density. The experiment of Ref. 28 was carried out at an electron energy $E = 500$ MeV, well above the threshold. The working medium was pure gaseous helium at standard temperature and pressure in a cell of length $T = 140$ cm. The spectral intensity of the radiation is seen to have a clearly defined maximum, whose height corresponds to and is proportional to the maximum value of the ratio of the absorption length to the coherence length for Cherenkov radiation, $(l_{coh}/l_c)_{max}$. This ratio, like the maximum of the spectral radiation intensity, is essentially independent of the density of the medium (its pressure) for electron energies well above the threshold. The apparent reason for the small quantitative difference between the theoretical and experimental spectral densities at wavelengths $\lambda \approx 800$ Å is that the absorption length was calculated for the case in which the photon interacts with an isolated helium atom. At standard pressure at wavelengths $\lambda \approx 800$ Å, however, an additional channel for photon absorption arises. This channel involves the

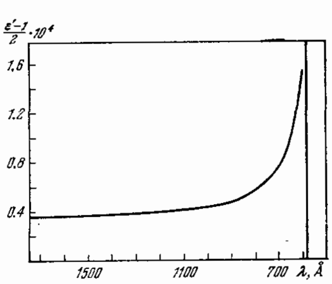

FIG. 1. Real part of the dielectric permittivity of helium vs the wavelength under standard conditions.[27]

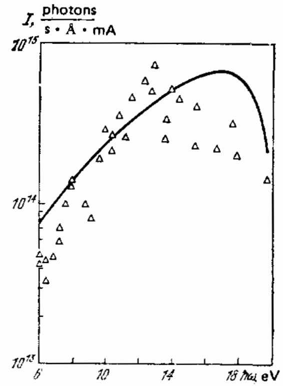

FIG. 2. The number of photons per unit wavelength interval, per unit current, in the Cherenkov radiation by electrons over a path 140 cm long in helium. Points—experimental; curve—calculated.[28]

formation of an excited helium dimer[39] through the three-body collision

$$\hbar\omega + \mathrm{He} + \mathrm{He} \rightarrow \mathrm{He}_2^*.$$

At high densities, this additional absorption channel may also be reflected in the real part of the dielectric permittivity at wavelengths $\lambda \approx 800$ Å, since the oscillator strength of the closest absorption line of the isolated helium atom, $\lambda_i = 584$ Å, begins to vary in a nonlinear way with the gas pressure.

The angular distribution of the radiation under the experimental conditions of Ref. 28 was determined by the multiple scattering of electrons over a 140-cm path in helium.

Since the inequality $(\varepsilon' - 1)/\varepsilon'' > 10^2$ holds in this frequency range, it follows from (1.8) and (1.9) that the Cherenkov radiation in helium is an exceedingly intense source of ultraviolet radiation in comparison with a synchrotron source.

Figure 3 shows the results of a comparison of the spectral power density of the Cherenkov radiation ob-

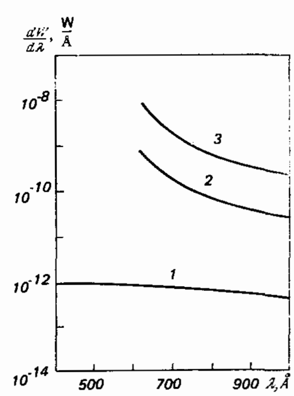

FIG. 3. Comparison of the spectral power density of the Cherenkov radiation from an electron in helium with the corresponding quantity for the radiation from the NBS synchrotron with an electron energy of 180 MeV (Ref. 28). 1—Synchrotron radiation; 2, 3—Cherenkov radiation at respective pressures of 1 and 10 atm.

served at wavelengths $\lambda \sim 2000 - 600$ Å with synchrotron radiation. We see that the intensity ratio reaches four orders of magnitude.

c) X-ray Cherenkov radiation

The possibility of x-ray Cherenkov radiation follows from the existence of anomalous-dispersion regions in materials, near the photoabsorption edges of electrons in inner atomic shells. Analytic expressions for $\varepsilon'(\omega)$ can be derived for these frequency regions from the Kramers-Kronig relation and from the known expressions for the cross section for the photoelectric effect (see Ref. 40, for example). Such calculations, however, are not very accurate, since they ignore the fine structure of the photoabsorption edge caused by the excitation of inner-shell electrons to free optical levels.[1)] Furthermore, the analytic form of the cross section for the photoelectric effect itself has only a finite accuracy.[42] Accordingly, more reliable results on $\varepsilon'(\omega)$ near the photoelectric-effect edges are found through numerical calculations from the dispersion formula and from the experimental values of the photoabsorption cross section over a broad frequency range.[43,44]

Experiments have been carried out for certain materials in which an x-ray interferometer was used to determine directly the real part of the dielectric permittivity near photoabsorption edges.[45] These measurements showed that $\varepsilon'(\omega)$ near the photoabsorption edges is higher than the value calculated from the "plasma" formula $\varepsilon' = 1 - (\omega_p^2/\omega^2)$. Unfortunately, the data correspond to elements and shells for which $\chi'(\omega) = \varepsilon'(\omega) - 1$ remains negative.

The results calculated for $\varepsilon'(\omega)$ for several materials with the dispersion formula

$$\varepsilon'(\omega) - 1 = \frac{2}{\pi} \int_0^\infty \frac{x\varepsilon''(x)}{x^2 - \omega^2}\, dx$$

and from experimental data on the photoabsorption cross sections[43,44] were published in Refs. 29 and 30. A criterion for the validity of the calculations was a simultaneous satisfaction of the Thomas-Reiche-Kuhn sum rules.[42] Curve 1 in Fig. 4 shows results calculated for the real part of the dielectric permittivity for carbon, along with values of $\varepsilon''(\omega)$ (curve 2) in the corresponding frequency range. It turns out that for several materials[30] the real part of the dielectric permittivity is greater than unity in comparatively narrow frequency intervals in the x-ray and UV ranges, near the photoabsorption edges of electrons in inner atomic shells.

The sepctral energy density of the Cherenkov radiation from a semi-infinite slab (of various materials, specified in the figures) was calculated from (1.5) in Refs. 29 and 30. As mentioned above, the properties

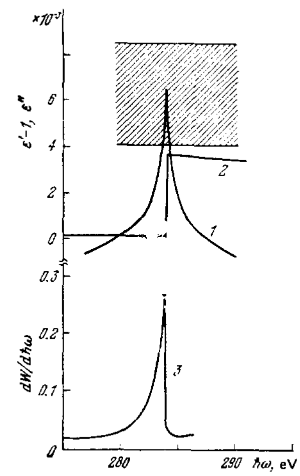

FIG. 4. The dielectric permittivity of carbon (1 and 2) and the spectral energy density of the Cherenkov radiation from a carbon layer (3) vs the photon energy.[29,30]

of this radiation are similar to those of Cherenkov radiation if $v\sqrt{\varepsilon'} > c$ and $\varepsilon' - 1 \gg \varepsilon''$. Frequency intervals in which the latter condition hold exist for all the materials in Figs. 4 and 5.

Figure 5 shows the spectral energy density of the emission by an electron with an energy $E = 1$ GeV, which lies above the threshold for several materials. Curve 3 in Fig. 4 shows the detailed emission spectrum in carbon near the threshold for the photoelectric effect. The spectral energy density of the emission from a semi-infinite slab has a sharper peak than that in the Cherenkov radiation in the UV region, in accordance with the behavior of the ratio of the real and imaginary parts of the susceptibility $[\varepsilon'(\omega) - 1]/\varepsilon''(\omega)$.

The spectral-angular emission density in (1.4) is a function of two variables: the emission frequency ω and the angle (θ) between the electron velocity and the emission direction. Curve 2 in Fig. 6 (Ref. 30) shows the spectral-angular energy density of the emission as

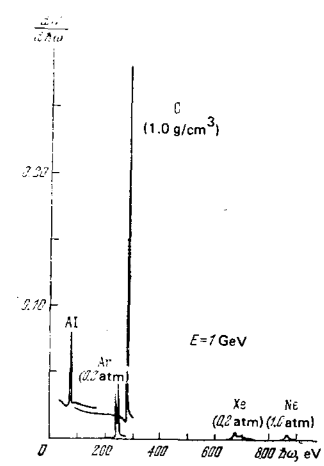

FIG. 5. Spectral energy density of the Cherenkov radiation by a 1-GeV electron from thick layers of various materials vs the photon energy.[30]

[1)]In particular, in this approch $\varepsilon'(\omega)$ formally has a discontinuity at the threshold for the photoelectric effect, and one may reach the erroneous conclusion[41] that Cherenkov radiation can occur near the photoelectric-effect edge in any material.

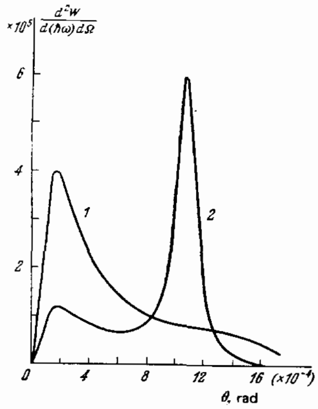

FIG. 6. Spectral-angular energy density of the radiation from a thick layer of argon at a pressure of 0.2 atm vs the emission angle.[30] 1—Photon energy $\hbar\omega = 248.4$ eV; 2—$\hbar\omega = 245.4$ eV.

a function of θ at the fixed frequency $\omega = 245.4$ eV, which corresponds to the maximum intensity of the Cherenkov radiation in argon. This curve has two clearly defined peaks, at angles $\theta_{tr} \approx \gamma^{-1}$ and $\theta_0 = \sqrt{\varepsilon' - 1 - \gamma^{-2}}$, corresponding to transition radiation and Cherenkov radiation. The angular width $\Delta\theta$ of the Cherenkov peak is determined by the diffraction angle over the absorption length $l_c(\omega)$ and amounts to $\Delta\theta = \varepsilon''(\omega)/\sqrt{\varepsilon'(\omega) - 1 - \gamma^{-2}}$. The ratio of the angular width to the emission angle is equal to the ratio of the coherence length for the Cherenkov radiation to the photoabsorption length, $\varepsilon''/(\varepsilon' - 1 - \gamma^{-2})$. For the frequency corresponding to curve 2 in Fig. 6, the maximum of the spectral-angular density of the Cherenkov radiation (at $\theta = \theta_0$) exceeds the maximum of the transition radiation (at $\theta = \theta_{tr}$). For the other frequency $\omega = 248.4$ eV, for which the ratio $l_c(\omega)/l_{coh}(\omega)$ is comparable to unity (curve 1 in Fig. 6), most of the radiation occurs at angles near θ_{tr}. These results illustrate the relationship between the Cherenkov and transition radiation as a function of the parameter l_c/l_{coh}. Figure 7 illustrates the threshold characteristics of the Cherenkov radiation by electrons in the x-ray range.

The possibility of Cherenkov radiation in the x-ray range is of considerable practical interest, since in this range the spectral-angular density of the Cherenkov radiation (per electron) can run to more than two orders of magnitude above the corresponding value for synchrotron radiation [see Eq. (1.8)], and the spectral energy density of Cherenkov radiation is more than an order of magnitude greater than the corresponding value for synchrotron radiation [see Eq. (1.9)].

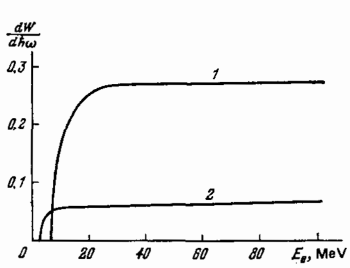

FIG. 7. Threshold characteristics of the Cherenkov radiation.[63] These curves show the spectral energy density of the radiation vs the electron energy for various materials, for fixed photon energies $\hbar\omega$ [for which $(\varepsilon' - 1)/\varepsilon''$ reaches its maximum]. 1—Radiation in carbon ($\rho = 1$ g/cm^3) at $\hbar\omega = 283.96$ eV; 2—in aluminum ($\hbar\omega = 72$ eV).

Another distinguishing feature of the Cherenkov radiation in the x-ray range is the relatively small spectral width $\Delta\omega, \lesssim 1$ eV. Cherenkov radiation in the x-ray frequency range is thus quite intense and monochromatic.

The Denisov group[46] has recently obtained the first experimental confirmation of the Cherenkov effect in amorphous carbon (density of 1.75 g/cm^3, plate thickness of 200 μm) at frequencies near the K edge of the photoelectric effect. This experiment was carried out on the LUÉ-2 linear electron accelerator of the Khar'kov Physicotechnical Institute ($E = 2$ GeV). A relative measurement of the spectral intensity of the radiation not only provided experimental confirmation of the Cherenkov radiation predicted in Ref. 29 but also yielded the maximum value of the extent to which $\varepsilon'(\omega)$ exceeded unity: $4.05 \times 10^{-3} < (\varepsilon' - 1)_{max} < 8.54 \times 10^{-3}$. The calculated value[30] of $(\varepsilon' - 1)_{max}$ which is $6.77 \cdot 10^{-3}$ (Fig. 4) lies within this interval (the hatched region).

d) Cherenkov emission of γ rays

Near an isolated line of a Mössbauer nuclear transition whose frequency (ω_{12}) is much higher than the frequency of the K-electron motion, the dielectric permittivity is

$$\varepsilon(\omega) - 1 = -\frac{-\omega_p^2}{\omega^2} + \frac{N\sigma_0}{(1-\alpha)\,\omega} f_L \frac{\Gamma\, 2}{\omega_{12} - \omega - (i\Gamma/2)}, \tag{1.10}$$

where $\sigma_0 = 2\pi\lambda\!\!\!^{-}{}_{12}^2(2I_2 + 1)/(2I_1 + 1)$ is the photon absorption cross section at the center of the line, $\lambda\!\!\!^{-}{}_{12} = c/\omega_{12}$, I_1 and I_2 are the angular momenta of the nucleus in its initial and excited states, α is the internal-conversion coefficient, Γ is the natural line width, and f_L is the probability for recoillness photon emission (the Lamb-Mössbauer factor). For non-Mössbauer transitions, the operation of averaging the right side of (1.10) over the shift of the resonant frequency ω_{12} reduces by many orders of magnitude the contribution of the nuclear absorption line to $\varepsilon'(\omega)$, since the Doppler line width is much greater than the homogeneous width Γ of a nuclear-transition line. The positive contribution to $\varepsilon'(\omega)$ made by the interaction with nuclei reaches a maximum value at the frequency $\omega = \omega_{12} - (\Gamma/2)$. According to the results of Ref. 31, for the transition $\hbar\omega_{12} = 14.4$ keV in the iron isotope Fe^{57} ($\Gamma/\omega \approx 3.3 \times 10^{-13}$) there is a frequency region near $\bar{\omega}$, of width $\Delta\omega \approx 5 \times 10^{-8}$ eV, in which the contribution to $\varepsilon'(\omega)$ from the interaction of photons with nuclei exceeds the negative contribution from the interaction with electrons, and the necessary condition for Cherenkov radiation, $v > c/\sqrt{\varepsilon'}$, can be satisfied. Figure 8 shows the behavior of $\varepsilon'(\omega) - 1$ and that of ε'' near the line of the Mössbauer transition in Fe^{57}, along with the spectral energy density of the Cherenkov radiation by an electron ($E = 1$ GeV) according to Eq. (1.5) (see also Ref. 47). We see from this

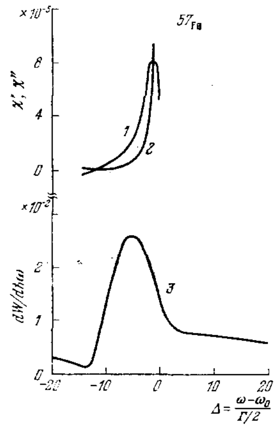

FIG. 8. Frequency dependence of the dielectric permittivity ($1-\chi'$; $2-\chi''$) and of the spectral energy density of the radiation by 1-GeV electrons (3) for Fe^{57} (12Kh18N10T steel) at 77 K ($\hbar\omega_{12} = 14.39$ keV).

figure that the parameter χ'/χ'' can reach a value of five in a narrow frequency interval. At electron energies above the threshold (200–300 MeV), the intensity of the Cherenkov radiation in this range is thus much higher than that of synchrotron radiation [see Eqs. (1.8) and (1.9)].

According to Refs. 31 and 47–49, Cherenkov radiation near lines of a Mössbauer nuclear transition can also occur in other isotopes.

2. RADIATION IN ARTIFICIAL PERIODIC STRUCTURES

The transition radiation in the x-ray range which occurs at one interface between materials having different dielectric properties is extremely faint. As the number of boundaries increases, however, interference effects can occur and substantially intensify the radiation in certain frequency and angular intervals. Such effects occur when the dielectric properties of the medium vary periodically over space with a period equal to the coherence length of the x-ray transition radiation. This case was first analyzed in detail by Ter-Mikaelyan,[50] although the problem of radiation in a layered medium had been treated in its general form earlier by other investigators[50–54] (see also the review in Ref. 55). Ter-Mikaelyan called the coherent transition radiation "resonance radiation."

Resonance radiation has much in common with Cherenkov radiation; in particular, in both cases there are a threshold and a characteristic directionality. The resonance radiation in the x-ray range is thus frequently also called "parametric Cherenkov radiation" or "quasi-Cherenkov radiation." The similarities are not simply fortuitous; they result from the fact that under certain conditions a medium with periodic dielectric properties can be characterized by a certain set of effective dielectric permittivities, which may exceed unity over a broad range of x-ray frequencies.[56] We will demonstrate this point with some simple arguments based on energy and quasimomentum conservation in the case of emission in a periodic medium. We denote by ΔE and Δp, respectively, the changes in the energy and momentum of the electron upon emission, by $\hbar\omega$ and $\hbar\mathbf{k}$ the energy and momentum of the emitted photon, by T the period of the medium, and by $\varepsilon_0(\omega)$ the dielectric permittivity averaged over a period. The conservation laws can then be written

$$\Delta E = \hbar\omega, \quad \Delta\mathbf{p} = \hbar\mathbf{k} - \frac{2\pi\hbar}{T}\mathbf{n}r. \tag{2.1}$$

Here we have taken into account the fact that upon emission the photon may transfer to the medium a momentum equal to a multiple of the reciprocal-lattice vector $\mathbf{K} = (2\pi/T)\mathbf{n}$, where n is the direction of the periodic change in the dielectric permittivity, and $r = 0, \pm 1, \pm 2, \ldots$. We assume for simplicity that the electron velocity v lies along the direction of n. During the emission of relatively soft photons, we have $\Delta E \approx \Delta\mathbf{p}\cdot\mathbf{v}$, and the relation between the frequency and angle of photon emission becomes[50,56]

$$\omega\left(1 - \frac{v\sqrt{\varepsilon'(\omega)}}{c}\cos\theta\right) = \frac{2\pi v}{T}. \tag{2.2}$$

We now make use of the fact that the average susceptibility in the x-ray frequency range, $\chi_0(\omega) = \varepsilon_0(\omega) - 1$, and the effective emission angles are small, while the period of the medium, T, is much larger than the radiation wavelength $\lambda = 2\pi c/\omega$ in cases of practical interest. Expression (2.2) can thus be rewritten in the form

$$1 - \frac{v}{c}\sqrt{\varepsilon'_{eff}(r, \omega)}\cos\theta = 0, \tag{2.3}$$

where $\varepsilon'_{eff}(r, \omega) = \varepsilon'_0(\omega) + 2\lambda(r/T)$ is the effective dielectric permittivity corresponding to radiation in the r-th harmonic. It is easy to see that for positive values of r the quantity $\varepsilon_{eff}(r, \omega)$ may exceed unity, giving rise to the possibility of resonance x-ray emission by an electron of sufficiently high energy:

$$E > E_{th}(r) = \frac{mc^2}{\varepsilon'_{eff}(r, \omega) - 1}. \tag{2.4}$$

By analogy with Cherenkov radiation [see (1.2)] we can define a coherence length for resonance radiation:

$$l_{coh}(r, \omega) = \frac{\lambda}{\varepsilon'_{eff}(r, \omega) - 1 - \gamma^{-2}}. \tag{2.5}$$

It is natural to consider the case in which the photon absorption length $l_c(\omega)$ is much longer than the period of the material. In this case the coherence length for the resonance radiation, (2.5) is much smaller than the photon absorption length. The spectral energy density of the radiation emitted from a target of thickness $T \gg l_c$ in this case can be written in a form analogous to the Frank-Tamm formula [see Eq. (1.6) and the accompanying text][56]:

$$\frac{dW}{d\hbar\omega} = \frac{e^2}{\hbar c}\sum_{r=r_{min}}^{r=r_{max}} P_r \frac{\varepsilon'_{eff} - 1 - \gamma^{-2}}{\varepsilon''(\omega)}\eta(\varepsilon'_{eff}(r, \omega) - 1 - \gamma^{-2}). \tag{2.6}$$

Here P_r is the probability for the transfer of a momentum $(2\pi\hbar/T)r$ to the medium as a whole. In the derivation of (2.6), the maximum and minimum harmonic indices of the radiation, $r_{max} > 0$ and $r_{min} < 0$, were chosen under the condition that the effective dielectric permittivity remains approximately equal to unity.[50,56] Since the values of P_r fall off rapidly with increasing $|r|$ (more on this below), a more accurate determination of r_{max} and r_{min} is of little use. The effective angles of the resonance radiation are thus assumed to be small, as they essentially always are in the x-ray frequency range.

Let us assume that the dielectric permittivity of a material in the x-ray frequency range can be described by

$$\varepsilon(\omega, x) = \varepsilon_0(\omega) + \varepsilon_1(\omega, x),$$

where $\varepsilon_0 - 1 \ll 1$ and where the periodic component, $\varepsilon_1(\omega, x)$, is much smaller than unity and thus smaller than the constant component. The probabilities P_r can thus be written in the form[56]

$$P_r = \left| \frac{1}{T} \int_0^T \exp\left[\frac{i\omega}{2c} \int_0^x \varepsilon_1(\omega, x)\, dx \right] \exp\left(-\frac{2\pi r x}{T} \right) dx \right|^2. \qquad (2.7)$$

In particular, when $\varepsilon_1(\omega, x)$ varies in accordance with $\varepsilon_1(\omega, x) = \Delta \cos(2\pi x/T)$, the probabilities can be expressed in terms of the Bessel functions[50,56] J_r:

$$P_r = J_r^2\left(\frac{\omega T \Delta}{4\pi c} \right).$$

This is essentially the case when, for example, an intense ultrasonic wave propagates through a homogeneous medium.

Another important case is that of a layered medium consisting of plates with different dielectric permittivities $\varepsilon_a(\omega)$ and $\varepsilon_b(\omega)$ and thicknesses a and b. The probabilities P_r for a layered medium were calculated in Ref. 50b:

$$P_r = \left(\frac{\omega T}{2c} \Delta\varepsilon \right)^2 \left(\frac{\omega b}{2c} \Delta\varepsilon + 2\pi r \right)^{-2} \left(\frac{\omega a}{2c} \Delta\varepsilon - 2\pi r \right)^{-2} \times 4 \sin^2\left[\frac{a}{2T} \left(\frac{\omega b}{2c} \Delta\varepsilon + 2\pi r \right) \right], \qquad (2.8)$$

where $\Delta\varepsilon = \varepsilon_a(\omega) - \varepsilon_b(\omega)$ is the abrupt change in the dielectric permittivity, and $T = a + b$ is the period of the medium.

Since the probabilities P_r satisfy the condition $\sum_r P_r = 1$, the inequality $P_r < 1$ holds. Deviations from a strict periodicity give rise to an effective decrease in the P_r. If these deviations are relatively small, their effect on the resonance radiation can be taken into account by introducing factors of the form

$$f(r) = \exp\left[-\frac{(\Delta T)^2}{T^2} (2\pi r)^2 \right] \qquad (2.9)$$

in (2.7), where $(\Delta T)^2$ is the mean square deviation of the period from its mean value; this was shown by Ter-Mikaelyan.[50] Furthermore, when deviation from strict periodicity is taken into account we find an incoherent background of transition radiation, corresponding to the independent emission by an electron in each period of the structure.

With increasing index of the resonance-radiation harmonic, the conditions imposed on the quality of the periodic structure become more stringent. As the deviations from periodicity increase ($\Delta T \to T$), the coherence effects disappear, and the spectral-angular characteristics of the transition radiation are determined by a simple sum of the intensities from the various interfaces.

The effect of an irregularity of the medium on the emission spectrum was analyzed in detail by Garibyan *et al.*,[57] who derived results for an arbitrary layered medium. The same investigators simultaneously examined the effect of absorption on coherence effects in transition radiation. Zhevago[56] took a different approach to incorporate absorption in an arbitrary, strictly periodic medium. A more complex question is that of the effect of multiple scattering on resonance radiation, since in a rigorous approach it is necessary to consider the periodic change in the mean square multiple-scattering angle caused by a change in the density of the material. If multiple scattering is taken into account only on the average (i.e., if the distribution of nuclei in the medium is assumed homogeneous), then the problem can be solved comparatively simply.[50,56] As Garibyan and Yan Shi[58,59] have shown, however, for the case of a layered medium, the incorporation of a periodic change in the multiple-scattering angle can have significant effects in the coherent transition radiation. We will not discuss this question in detail; we simply note that when the inequality

$$\frac{q\lambda}{(\varepsilon'_{eff} - 1 - \gamma^{-2})^2} \ll 1 \qquad (2.10)$$

[analogous to inequality (1.3)] holds we can ignore the effect of multiple scattering on the resonance radiation.

We turn now to some specific estimates of the spectral density of the resonance transition radiation. In the x-ray frequency range, the dielectric susceptibility $\varepsilon'(\omega) - 1$ is proportional to the atomic number Z of the material, while the absorption $[(\varepsilon''(\omega)]$ increases more rapidly with increasing Z. From the standpoint of the emission yield, therefore, a medium with a value of Z as low as possible is the optimum choice. As an example we consider a medium consisting of 750 layers of beryllium $2.5 \cdot 10^{-3}$ cm thick, separated by vacuum gaps 0.05 cm thick. For such a medium we have $P_1 \approx 0.4$; and $(\varepsilon' - 1)/\varepsilon'' \approx 2 \cdot 10^3$ at $\omega = 15$ keV ($\lambda \approx 0.83$ Å). The threshold energy for first-harmonic generation is $E_{th}^{(1)} = 1.5$ GeV. The spectral energy density of the radiation at the frequency $\omega \approx 15$ keV and at electron energies above the threshold is

$$\frac{dW_m}{d\hbar\omega} \approx 10.9. \qquad (2.11)$$

The spectral and spectral-angular density of the resonance radiation per electron at x-ray frequencies may thus exceed the corresponding values for synchroton radiation over a coherence length by nearly four orders of magnitude. Consequently, as mentioned by Zhevago,[56] the transition radiation in periodic structures may be of interest for developing an x-ray source.

Many experimental studies of the transition radiation in layered structures have been published.[60-79] The primary motivation for this work was the goal of using x-ray transition radiation to detect high-energy charged particles. The most important characteristic for this application, however, is the total radiative energy loss by the particle in the radiator.[62,65,66,73,75]

TABLE II. Parameters of the layered structures (radiators) used in the experiments on transition radiation.[78]

Film material/material between films	Film thickness, cm	Distance between films, cm	Number of layers	Maximum radiation frequency, keV
$(CH_2)_n$/He	$1.6\cdot 10^{-3}$	0.14	1000	5.6
$(CH_2)_n$/He	$5.0\cdot 10^{-3}$	0.14	250	18
$(CH_2)_n$/He	$8.2\cdot 10^{-3}$	0.14	200	29
$(CH_2)_n$/air	$3.0\cdot 10^{-3}$	0.10	300	11
$(CH_2)_n$/air	$2.44\cdot 10^{-2}$	0 75	200	86
$(CH_2)_n$/air	$2.44\cdot 10^{-2}$	1.5	100	86

The spectral distribution of the radiation which arises in a regular layered medium has been studied by several groups of investigators.[60-62, 64, 66, 67, 71, 72, 74] As a rule, total-absorption spectrometers have been used to detect the photons in these experiments. On the other hand, the probability for the emission of two or more photons in the radiators has been substantial. Since the procedure used to detect the radiation does not allow one to distinguish between the emission of a single photon and that of several photons, the accuracy of the spectral measurements was inadequate.[77] An exceptional case is represented by the experiments by Fabjan and Struczinski,[74] who used a radiator with a relatively large number of layers (≈30), and where the probability for the emission of more than a single photon was relatively low. An agreement within 15% with the theoretical predictions was achieved in those experiments.[74-76]

The most thorough study of the spectral characteristics of transition radiation in various layered media has been carried out by Cherry and Müller.[77,78] Their experiments were carried out on the synchrotron at Cornell University for electron energies of 5, 9, and 30 GeV. Table II shows the parameters of the layered structures used as radiators. Some of the results are shown in Fig. 9 as emission spectra. The quantity plotted along the ordinate is the number of photons emitted in a unit energy interval per electron, per period of the medium. The experimental values (shown by the circles and the triangles) agree within 15% with the theoretical curves.

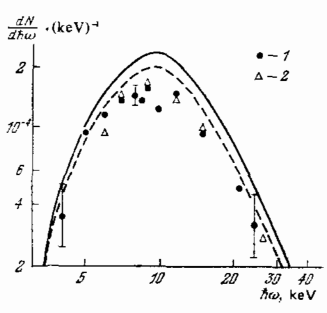

FIG. 9. Photon-energy dependence of the number of photons emitted by an electron in a multilayer medium consisting of 1000 polypropylene films, 16 μm thick, separated by 1.4-mm helium-filled gaps. The results are expressed in terms of the number of photons per boundary. 1—Experimental results for 5-GeV electrons; 2—experimental results for E = 9 GeV (Ref. 78); solid and dashed curves—respective theoretical spectra.

According to these results, the spectral energy density of the radiation in the radiators per electron, $dW/d\hbar\omega$, reaches a value of 1.6, which is nearly three orders of magnitude higher than the corresponding value for synchrotron radiation.

Transition radiation in periodic structures may thus be regarded as a potential source of intense x radiation.

3. RADIATION IN A CRYSTAL WHICH RESULTS FROM THE DIFFRACTION OF VIRTUAL PHOTONS

A single crystal is a naturally occurring periodic structure but the spatial period of the variations in the dielectric properties of the crystal may be comparable to the wavelengths of the x radiation. In contrast with the artificial structures discussed above, therefore, calculations of the emission spectra in a crystal must generally incorporate the interaction of the electromagnetic field of the charge with the individual atoms. This approach is used, in particular, in the theory of x-ray diffraction in crystals.[81-83]

The self-field of a relativistic electron has properties similar to that of an electromagnetic wave. The resonance (or quasi-Cherenkov) radiation in a crystal may thus be regarded as a result of the diffraction of the field of the moving electron, i.e., as a coherent scattering of the virtual photons by atoms of the crystal. In complete correspondence with x-ray diffraction, we may distinguish two cases in the emission.

The first case corresponds to the conditions for "kinematic" diffraction, under which the intensity of the diffracted wave remains small in comparison with the intensity of the direct wave at all times. Ter-Mikaelyan[50b] (§28) has carried out calculations for all the radiation spectrum of a charge in uniform motion in a crystal for this case. Belyakov[84] has derived some corresponding results, taking the thermal vibrations of the crystal atoms into account.

In thick crystals the intensities of the direct and diffracted waves may be comparable in magnitude, and it may become necessary to consider the constant interaction of two (or more) waves in the course of the diffraction. This case corresponds to dynamic diffraction theory. A radiation theory based on the dynamic diffraction of the self-field of an electron has been derived by Garibyan, Yan Shi, *et al.*[85-87] Afanas'ev and Aginyan[88] have derived some comparatively simple analytic expressions for the spectra of the radiation emitted by an electron in a crystal. The same investigators have derived a theory for radiation in mosaic crystals. Baryshevskiĭ and Feranchuk[89,90] have also studied the emission by a particle in uniform motion in a single crystal, but their first results[89] turned out to be incorrect; as a result, the emission intensity was overestimated by many orders of magnitude. These errors were subsequently corrected.[90]

a) Emission in the case of kinematic diffraction

By virtue of the translational symmetry of a crystal, the space-time Fourier components of the electromagnetic field can be written as series in the reciprocal-lattice vectors K. For the electric field of an electromagnetic wave, for example, we find

$$\mathscr{E}(\mathbf{r},\ t)=v_c^{-1}\sum_{\mathbf{K}}\mathbf{E}_{\mathbf{K}}(\mathbf{k},\ \omega)\exp[i(\mathbf{k}_{\mathbf{K}}\mathbf{r}-\omega t)], \tag{3.1}$$

where $\mathbf{k}_K=\mathbf{k}+\mathbf{K}$, and v_c is the volume of the unit cell of the crystal. In this case Maxwell's equations for the field of the charge in the crystal reduce to a system of algebraic equations for the quantities $\mathbf{E}_K(\mathbf{k},\omega)$. The solution of this system of equations for the field of a charge moving at a velocity $\mathbf{v}$ in a crystal is, in the weak-diffraction approximation (Ref. 50b, §28),

$$\mathbf{E}_{\mathbf{K}\neq 0}(\mathbf{k},\ \omega)=\frac{8i\pi^2 e}{c^2}\,\frac{\omega^2c^{-2}\chi_{\mathrm{KO}}}{\omega^2c^{-2}\varepsilon_0-k^2}\,\frac{[\mathbf{k}_{\mathrm{K}}[\mathbf{k}_{\mathrm{K}}(\omega\mathbf{v}-\mathbf{k}\varepsilon_0^{-1}c^2)]]}{\omega^2c^{-2}\varepsilon_0-k_{\mathrm{K}}^2}, \tag{3.2}$$

where $\chi KO(\omega)$ are coefficients proportional to the amplitude for the scattering of a photon by a cell of the crystal with a change K in the photon momentum. In the case under consideration, the average dielectric permittivity ε_0 is determined by

$$\mathrm{Re}\,\varepsilon_0(\omega)=1+\chi_0',\quad \chi_0'=\frac{-\omega_p^2}{\omega^2}.$$

The imaginary part of $\varepsilon_0(\omega)$ can be expressed in terms of the photon absorption cross section $\sigma_c(\omega)$:

$$\mathrm{Im}\,\varepsilon_0(\omega)=\chi_0''=\frac{cn\sigma_c(\omega)}{\omega},$$

where n is the density of absorbers. The primary absorption mechanism in the x-ray frequency range is the photoelectric effect at atomic electrons, and the absorption is usually relatively weak, $\chi_0''\ |\chi_0'|$. For the other coefficients, the following relations can be derived[91] for the case of a monatomic crystal and for x-ray frequencies:

$$\chi_{\mathrm{KO}}'(\omega)=\chi_0'F(\mathrm{K})\exp[-W(\mathrm{K})]/Z,$$
$$\chi_{\mathrm{KO}}''(\omega)=\chi_0''\exp[-W(\mathrm{K})],$$

where $F(\mathrm{K})$ is an atomic structure factor $[F(0)=Z]$, Z is the number of electrons in the atom, and $W(\mathrm{K})$ is the Debye-Waller factor. In the Debye approximation we have $W(K)=K^2u^2$, where u^2 is the mean square amplitude of the thermal vibrations of the crystal atoms.

The approximate solution in (3.1) is valid at least when the wavelength of the emitted photon is substantially smaller than the dimensions of the unit cell of the crystal. Using the condition $k\gg K$, we can write the denominator of the last factor in (3.2) as[92]

$$\omega^2c^{-2}\varepsilon_0-k_{\mathrm{K}}^2\approx\omega^2c^{-2}\varepsilon_{\mathrm{eff}}(\omega,\ K_z)-k^2, \tag{3.3}$$

where $\varepsilon_{\mathrm{eff}}(\omega,K_z)=\varepsilon_0(\omega)-2K_z\omega^{-1}c$ is the effective dielectric permittivity of the crystal, and K_z is the projection of the reciprocal-lattice vector onto the velocity of the particle.

Quasi-Cherenkov radiation from an electron in a crystal arises at those electron energies and at those angles with respect to the velocity direction which correspond to the vanishing of the denominator in (3.3). It is not difficult to see that when diffraction is taken into account ($K_z\neq 0$) the latter condition can in fact hold if the particle energy lies above the threshold $E_{\mathrm{th}}(K_z)=mc^2[\varepsilon_{\mathrm{eff}}'(\omega,K_z)-1]^{-1/2}$. The expression[92] found for the spectral energy density of the radiation in a sufficiently thick crystal $[T\gg l_c(\omega)]$ is similar to that for a layered medium, (2.6):

$$\frac{dW}{d(\hbar\omega)}=\frac{e^2}{\hbar c}\sum_{K_z<0}P_K\frac{\varepsilon_{\mathrm{eff}}'(\omega,\ K_z)-1-\gamma^{-2}}{\varepsilon_0''(\omega)}\eta(\varepsilon_{\mathrm{eff}}'-1-\gamma^{-2}).$$

The summation, however, is now over a three-dimensional manifold of reciprocal-lattice vectors, and the factors P_K are

$$P_K=\frac{|\chi_{\mathrm{KO}}(\omega)|^2\omega^2}{4c^2K_z^2}.$$

These factors are proportional to the square of the small parameter $\lambda a/\lambda_p^2$, where λ is the emission wavelength, $\lambda_p=2\pi c/\omega_p$, and a represents the dimensions of the unit cell of the crystal. With increasing emission wavelength, the intensity of the quasi-Cherenkov radiation in the crystal rises. Under the condition $\lambda\sim a$, however, the perturbation method used in the calculations generally becomes inapplicable. Under this condition, *the method of dynamic diffraction theory is* more systematic.[85-87] In discussing this question we will follow Afanas'ev and Aginyan.[88]

b) Radiation in the case of dynamic diffraction

We assume that the Bragg condition holds: $k^2\approx k_1^2$, where $\hbar k\approx\hbar\omega c^{-1}$ is the momentum of the virtual photon of the electron field, $\hbar\mathbf{k}_1=(\mathbf{K}_1+\mathbf{k})\hbar$ is the momentum of the emitted photon, and $\mathbf{K}_1$ is some fixed reciprocal-lattice vector. In this case, of all possible Fourier components of the field the only significantly nonzero ones are the components of E_0, and of $\mathbf{E}_{\mathbf{K}_1}\equiv\mathbf{E}_1$. The system of equations for the Fourier components of the field can thus be reduced[88] to a system of two equations for the vectors E_0 and $\mathbf{E}_1$.

In this approximation, the solution of the system of equations for the components of a field propagating at the Bragg angle is[88]

$$E_1^{(s)}=\frac{8i\pi^2ev}{\omega}\chi_{10}P^{(s)}c^{(s)}\delta(\omega-\mathbf{kv})/\Delta^{(s)}, \tag{3.4}$$

where $\Delta^{(s)}=\chi_{01}\chi_{10}c_s^2-\bar{\chi}_0(\bar{\chi}_0-\alpha)$ $\alpha=(K_1^2-k^2)c^2/\omega^2$, $\bar{\chi}_0=\chi_0-\gamma^{-2}-\theta^2$; $\chi_{10}=\chi_{01}=\chi_{\mathbf{K}_1\mathrm{O}}$; γ is the Lorentz factor of the moving electron; θ is the angle between the momentum of the virtual photon and the velocity vector; $c^{(s)}$ are constants which depend on the direction of the field polarization vector $\mathrm{e}^{(s)}$,

$$c^{(s)}=\begin{cases}1 & \text{— for the } \sigma \text{ polarization,}\\ \cos 2\theta_B & \text{— for the } \pi \text{ polarization;}\end{cases}$$

and $P^{(s)}=\mathrm{e}^{(s)}\varkappa/\varkappa$, where $\varkappa$ is the component of the momentum of the virtual photon which is perpendicular to the velocity of the particle (for the case of relativistic particles, the effective values of $\varkappa$ are relatively small, $\varkappa\ll k$). The quasi-Cherenkov (dynamic) emission occurs when the electron velocity exceeds the phase velocity for the propagation of electromagnetic waves in the crystal. The corresponding frequencies and directions of the emission are determined by the condition that the real part of the denominator vanishes:

$$\mathrm{Re}\,\Delta^{(s)}\approx(\gamma_{01}'c^{(s)})^2-\tilde{\chi}_0'(\tilde{\chi}_0'-\alpha). \tag{3.5}$$

It is not difficult to show that for emission at an angle of $2\theta_B$ with respect to the direction of the electron velocity the quantity in (3.5) vanishes for the frequency $\omega_0 \approx Kc/2\sin\theta_B$. Slight deviations from this direction lead to a corresponding change in the emission frequency, $\Delta\omega = \omega - \omega_0$. Since the absorption of the radiation is relatively weak ($\chi_0'' \ll \chi_0'$), there is a nearly unambiguous correspondence between the emission frequency and the emission direction:

$$\sin\theta_B \frac{\Delta\omega}{\omega_0} \approx \theta\cos\varphi\cdot\cos\theta_B.$$

The angle φ is measured from the plane formed by the vectors $\mathbf{v}$ and $\mathbf{K}$, and the angle θ is measured from the direction of the vector $(\omega_0\mathbf{v}/v)+\mathbf{K}$. The spectral-angular distribution of the emission intensity in the Bragg direction ($\theta_B < \pi/2$) for a sufficiently thick crystal is determined by

$$\frac{d^2W}{d(\hbar\omega)\,d\Omega} = \frac{16\pi^3 e^2}{\hbar c}\sum_{S=\sigma,\pi}\frac{|P^{(s)}c^{(s)}\chi_{10}|^2}{\rho^{(s)}(\theta)\sin^2\theta_B}\,\delta\left(\frac{\Delta\omega}{\omega_0} - \theta\cos\varphi\,\mathrm{ctg}\,\theta_B\right),$$

$$\rho^{(s)}(\theta) = c^{(s)2}\chi_{01}'(2\chi_{01}''\tilde{\chi}_0' - \chi_0''\chi_{01}') - \chi_0''\tilde{\chi}_0'^2. \tag{3.6}$$

The method of the dynamic theory of the diffraction of virtual photons for a crystal of arbitrary thickness can be used to calculate the radiation intensity and the frequency distribution within the emission line. For order-of-magnitude estimates, however, simpler qualitative methods are sufficient. As mentioned above, the dynamic radiation may be regarded as a result of an interference between the transition-radiation fields generated by the particle as it crosses atomic planes. The spectral-angular energy density of the transition radiation at a single plane at a sufficiently large angle $\theta \gg mc^2/E$ with respect to the direction of the velocity of a relativistic particle is given by (see Ref. 22, for example)

$$\frac{d^2W}{d(\hbar\omega)\,d\Omega} \sim \frac{e^2}{\hbar c}\frac{(\chi_0')^2}{\pi^2}.$$

The coherence of the radiation fields gives rise to an increase in the spectral-angular density in the Bragg direction; this increase is proportional to the square of the number of atomic planes over the radiation absorption length. In other words, for wavelengths of the order of the lattice constant, the increase is proportional to χ''^{-2}. As a result we obtain an estimate of the spectral-angular energy density of the radiation from the crystal at the Bragg angle:

$$\frac{d^2W}{d(\hbar\omega)\,d\Omega} \sim \frac{e^2}{\pi^2\hbar c}\left(\frac{\chi_0'}{\chi_0''}\right)^2.$$

The ratio χ'/χ'' reaches a value of the order of 10 in the x-ray frequency range. The spectral-angular density of this type of radiation is thus two orders of magnitude higher than that for synchrotron radiation. The radiation is relatively monochromatic ($\Delta\omega/\omega \sim 10^{-2}$). These estimates agree with more accurate calculations by Aginyan and Yan Shi[87] from Eqs. (3.6) for a LiH crystal.

The quasi-Cherenkov (dynamic) radiation in a crystal is thus interesting as a source of monochromatic x radiation with a tunable frequency. The tuning is achieved by varying the direction of the electron with respect to a reciprocal-lattice vector. Unfortunately, there has been no experimental study of this type of radiation.

4. RADIATION IN THE CASE OF CHANNELING OF PARTICLES IN CRYSTALS

If a charged particle enters a crystal at an angle with respect to a crystallographic axis or plane which is smaller than some critical angle θ_L, the particle may be channeled[93]: The particle may spend a relatively long time moving along the channels formed by the crystallographic planes or axes, where the potential energy of the interaction of the particle with the crystal is at a minimum. The scale dimension of the motion in the direction transverse to the channel is of the order of the interatomic distances. From the quantum-mechanical standpoint there are discrete energy levels which result from the finite transverse motion of the particles.[94]

Thompson[95] was the first to call attention to the possibility of spontaneous radiative transitions between the transverse-motion levels of protons as one of the effects which cause a change in the populations of the levels. Thompson believed that the radiation should occur in the infrared part of the spectrum, and a more detailed analysis has shown that nonrelativistic channeled protons can in fact emit infrared radiation upon transitions between transverse-energy levels. Unfortunately, this emission is relatively faint and extremely difficult to detect against the background of other radiation effects. It was probably for this reason that Thompson's idea was not pursued for a long time.

Kalashnikov *et al.*[196a] subsequently took up the problem of the radiation by nonrelativistic electrons as they go from the transverse-energy continuum into the discrete spectrum in an effort to explain experiments on the radiation by nonrelativistic electrons. For nonrelativistic electrons, however, there are no transverse-energy levels and there is accordingly no channeling; ordinary electron diffraction does occur. Furthermore, the equations derived by Kalashnikov *et al.*[196a] do not in fact describe this emission process. It was shown later[119] that when a nonrelativistic particle, but one heavier than the electron, having a fixed transverse energy goes from the continuum to a bound state the emission should be monochromatic, in contradiction to the results of Ref. 196a.

Kumakhov[96,97] was the first to suggest intense x and γ radiation during the channeling of relativistic electrons and positrons. The theoretical results can be summarized as follows. Relativistic effects play a twofold role in the emission by channeled particles. The relativistic increase in the mass of a particle causes a decrease in the distance between adjacent transverse-energy levels, i.e., a decrease in the frequency of the transverse oscillations. On the other hand, because of the Doppler effect the energy of the emitted photon in this case is generally not equal to the difference between transverse-energy levels. The radiation becomes concentrated along the longitudinal-motion direction. The photons emitted in this direction correspond to the x-ray or γ range if the particles are moving at relativistic velocities.

With increasing particle energy E, the intensity of the dipole radiation integrated over frequency increases in proportion to E^2, while the characteristic radiation frequencies increase in proportion to $E^{3/2}$. The spectral intensity of the radiation is so high that it can significantly exceed that of other known radiation mechanisms.

On the other hand, A. Vorob'ev *et al.*[98] reached conclusions quite different from those of Ref. 97 in calculations incorporating only the relativistic mass increase (and ignoring the Doppler effect).

The studies by Kumakhov[96,97] and the discovery of the possibility that this new type of radiation[2)] might be used as an intense source of x and γ radiation and for research on crystals stimulated further theoretical work[92,99-141] and the first experiments.[142-151] In particular, the basic results of Refs. 96 and 97 were found a year later by some other investigators.[92,103,128,130] The study by Baryshevskii and Dubovskaya[138] is an exceptional case: They originally predicted[138] that the intensity of the radiation by an ultrarelativistic (1-GeV) particle during channeling should be comparable to that of transition radiation; this intensity would be much lower than estimates made by other investigators.[92,103,109,128,130] Some other characteristics of the radiation, the spectral-angular density, and the polarization as calculated in Ref. 138 were also at odds with the results found by other investigators.[92,103,109,128,130] In some later papers, Baryshevskii *et al.*[139] corrected some of the errors in Ref. 138 (see Ref. 127b for more details), but the dependence of the photon energy on the emission angle and the particle energy found by Baryshevskii *et al.*[139] remained incorrect (as was shown in Ref. 127b), because the Doppler effect was taken into account incorrectly.

Kumakhov, Beloshitskiĭ, and Wedell[99-109] developed the theory for dipole radiation by channeled particles further. A theory for stimulated radiation was also taken up in Ref. 102, and the problem of making use of this stimulated radiation to develop a tunable laser was studied.

The authors of the present review derived a quantum-mechanical theory for the radiation from channeled particles with relatively high energies, at which the dipole approximation is not valid.[92,112-122] It was also shown[92,103,112-114,117,118] that there are several effects which result from the influence of the frequency and spatial dispersion of the electromagnetic field in a crystal on the radiation from channeled particles.

The radiation emitted by above-barrier particles during planar quasichanneling was studied in the dipole approximation first by Akhiezer *et al.*[131,132] and later by some other investigators.[111,118,119,133b,135-137] Some more general results, incorporating nondipole radiation, in particular, were derived for this case by Glebov and the present authors[119] (see also Ref. 127b). A theory for the radiation emitted during axial quasichanneling was derived by Avakian *et al.*,[123] Yamamura and Ohtsuki,[124] Shul'ga,[133a] and Bazylev and Demura.[123b] Beloshitskiĭ and Kumakhov[126] derived a theory for the radiation in the transitional case between planar and axial channeling.

It was shown[96,97,92,115,130] that there is an analogy between the radiation during planar channeling and quasichanneling, on the one hand, and the well-known undulator radiation,[20a,199-205] on the other. Pursuit of this analogy proved fruitful in the development of a theory for the radiation by high-energy particles during channeling (more on this below). The basic results derived in the theory of undulator radiation by Ginzburg and Eidman,[199a,b] Korkhmazyan,[201] and Alferov *et al.*[202] were used in specific calculations of the radiation during planar channeling and quasichanneling.[111,130-132,135-137]

Several theoretical papers have appeared recently on effects intimately related to the emission accompanying channeling. The role played by the inverse effect of the radiation on the motion of the channeled particles was determined by Vedel' and Kumakhov[105,106] Bonch-Osmolovskiĭ and Podgoretskiĭ,[134] and the present authors.[116] Pantell[140] has calculated the cross section for the scattering of a laser beam by a beam of channeled particles. We have derived a more detailed theory for this effect and also a theory for stimulated scattering.[120,121] Eremeev and Kumakhov[141] have discussed the possibility of neutron production by making use of the radiation from channeled particles.

Several experimental studies have been carried out on the spectrum of the radiation emitted by channeled electrons and positrons.[143-151] These experiments have revealed a definite increase in the yield of relatively soft x or γ rays when the particles enter a crystal at an angle less than the critical channeling angle.

The state of theoretical and experimental research on the radiation accompanying channeling was summarized briefly in a review by the present authors at the international conference at Hamilton[118] (August 1979) and in the review by Wedell.[152]

We turn now to a more detailed examination of the basic theoretical results on the Kumakhov effect, and we will compare these results with the experimental data available.

a) Particle-crystal interaction potential during the channeling of relativistic electrons or positrons

The channeling of charged particles in crystals has been the subject of many theoretical and experimental studies (see, for example, the reviews in Refs. 93-95). As was shown first by Lindhard,[153] a particle which enters a crystal at a sufficiently small angle from a crystallographic axis undergoes totally coherent scattering by the various atoms of this axis. As a result, the effect of the resultant potential of the crystal atoms can be approximated very accurately by the effect of a potential averaged along the direction of the axis. The average potential depends only on the distance from the axis, so that the problem of analyzing the particle mo-

[2)] This radiation is sometimes called the "Kumakhov effect" (see the review in Ref. 152, for example).

tion in the crystal during axial channeling is simplified substantially. A similar approach can be taken when the particle enters the crystal at a sufficiently small angle from a crystallographic plane.[154] The average plane potential acting on a particle during planar channeling depends only on the distance from the plane.

The average potential is generally a periodic function of the transverse coordinates with a primary period equal to the distance between adjacent axes or planes. In most cases of interest, however, it is sufficient to consider the potential of only a single plane or a single axis in the case of electrons or the potential of the two closest planes or of several closest axes in the case of positrons. The reason is that in these cases we can ignore the penetrability of the potential barriers separating adjacent channels.[106,115,125]

The potential of an individual channel can be described analytically by making use of simple models for the potential of the crystal atoms and for the thermal lattice vibrations. Appleton *et al.*[156] have carried out calculations of this sort in the Moliere approximation[155] for an atomic potential and with isotropic thermal vibrations (Fig. 10). Corresponding calculations, but without thermal vibrations, can be carried out for other model atomic potentials.[94,127] The expressions derived for the channel potentials in this manner are still quite complicated for use in analytic calculations of the emission spectra of channeled particles. In most cases, however, these expressions can be approximated well by simpler expressions which make the problems analytically solvable and also yield quick estimates of the radiation frequency and intensity where needed. For planar channeling of positrons, for example, the potential is given in a first approximation by the parabola

$$U(x) = \frac{4U_0x^2}{d^2} \tag{4.1}$$

over nearly the entire channel (Fig. 10a). The anharmonic corrections to the potential in (4.1) are small and can be treated by perturbation theory.[106,129] For electrons, the average potential of a plane can be described quite accurately by[115,118,119,157,158] (Fig. 10b)

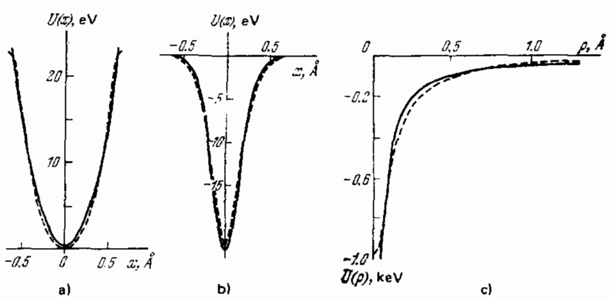

FIG. 10. Potentials of planar and axial channels.[118] The dashed curves are calculated from the Moliere model for the potential of the atom and incorporate the thermal lattice vibrations; the solid curves correspond to the simple model dependences in (4.1)–(4.3). a—Potential of the (110) planar channel of diamond for positrons; b—potential of the (110) planar channel of diamond for electrons; c—potential of the (111) axial channel of tungsten for electrons.

TABLE III. Parameters of the model potentials for certain crystals and channels.

Crystal		Plane		Axis	
Miller indices of axis or plane	Material	U_0, eV	b, Å	U_0, eV	α, eV·Å
	C	12.4	0.168	83	6.5
100	Si	13.1	0.245	88	8.5
	W	83.7	0.227	804	49
	C	22.8	0.215	101	9.0
110	Si	22.9	0.303	112	11.5
	W	132.8	0.275	553	34
111	C	—	—	99	7.0
	Si	—	—	104	9.5
	W	36.1	0.161	936	55

$$U(x) = -U_0 \operatorname{ch}^{-2}\frac{x}{b}. \tag{4.2}$$

and the potential of an axis by[99b,111,119,159,160] (Fig. 10c)

$$U(\rho) = -\frac{\alpha}{\rho}. \tag{4.3}$$

The parameters U_0, b, and α in (4.1)–(4.3) are chosen for the best fit of the models to the more accurate results.[156] Table III shows these parameters for some specific channeling situations. It is a more complicated problem to choose a model potential for axial channeling of positrons. In this case the potential generally is not cylindrically symmetric (see Fig. 8 in Ref. 94) and is difficult to write in any simple form.

b) Classical equations of motion of relativistic channeled particles

The motion of channeled particles in a crystal must generally be dealt with by quantum mechanics, since the de Broglie wavelength corresponding to the transverse motion (more on this below) may be comparable to the scale dimensions of the region of transverse motion. A classical description becomes possible, however, if the particles have sufficiently high energies. We will thus treat this high-energy case first, as the simplest. Some more precise conditions for the applicability of the classical approach will be formulated in Subsection 4c, where we will take up the quantum-mechanical theory of the motion.

The classical equations of motion of relativistic channeled particles are analyzed in Refs. 118 and 123a. We will follow Ref. 118 for our analysis of planar channeling.[3)]

For planar channeling, the longitudinal momentum component (longitudinal with respect to the planes), $p_\parallel$, and the total energy of the particle, E, are integrals of motion:

$$\frac{1}{\sqrt{1-v^2-(\dot{x})^2}} + U(x) = E, \qquad \frac{v_\parallel}{\sqrt{1-v_\parallel^2-(\dot{x})^2}} = p_\parallel. \tag{4.4}$$

Here $v_\parallel$ is the longitudinal velocity, and $\dot{x}$ is the transverse velocity of the particle. From system (4.4) we find

[3)] The equations of motion are analyzed in a system of units with $\hbar = m = c = 1$.

$$(\dot{x})^2 = \frac{[E - U(x)]^2 - E_\parallel^2}{[E - U(x)]^2}, \tag{4.5}$$

where $E_\parallel^2 = (p_\parallel^2 + 1)^{1/2}$ is the longitudinal energy. This is the exact equation of the transverse motion.

Equations (4.5) simplify further because the potential energy $U(x)$ is small in comparison with the total energy of the relativistic particle. We write the total energy as $E = E_\parallel + \varepsilon$, where ε is the transverse energy, and we note that for channeled particles we have $\varepsilon \sim U$ and thus $\varepsilon \ll E_\parallel$. Within quantities $\sim\varepsilon/E$ the equation of the transverse motion can thus be written

$$(\dot{x})^2 = \frac{2}{E_\parallel}[\varepsilon - U(x)]. \tag{4.6}$$

The equation of the transverse motion in (4.6) is thus nonrelativistic in form, but the mass of the particle in this equation is its relativistic mass $E_\parallel \approx E$.

The longitudinal velocity of a particle is determined by the second equation in system (4.4):

$$v_\parallel^2 = (1 - E_\parallel^{-2})(1 - (\dot{x})^2). \tag{4.7}$$

In the ultrarelativistic limit ($E \gg 1$) we find, using the condition $\varepsilon \ll E_\parallel$,

$$v_\parallel \approx 1 - \frac{1}{2}(E_\parallel^{-2} + (\dot{x})^2). \tag{4.8}$$

As the particle energy E increases, so does the accuracy of the equations of motion in (4.6) and (4.8). The transverse motion [Eq. (4.6)] and the longitudinal motion [Eq. (4.8)] of a channeled particle are coupled. This coupling is seen, on the one hand, in the parametric dependence of the transverse-oscillation frequency on the energy of the longitudinal motion, $E_\parallel$. On the other hand, at sufficiently high energies $E \sim 1/\varepsilon_{\text{kin}}$, where $\varepsilon_{\text{kin}} = (\dot{x})^2/2E$ is the kinetic energy of the transverse motion, the longitudinal oscillations of a particle become significant because of this coupling [see (4.8)]. Such oscillations strongly affect the emission spectrum.[118,119,127b] (see also Subsection 4j).

The results in (4.4)–(4.8), for planar channeling, can be extended to the case of axial channeling through the obvious substitution $x \to \rho$ (where ρ is the radius vector perpendicular to the channeling axis).[123]

c) Quantum equations of motion of relativistic channeled particles

We will derive the quantum equations of motion of particles in a channel, following the results of Refs. 92, 115, and 161.

The wave function $\Psi(\mathbf{r}, t)$ of a relativistic electron (or positron) in an external field is a bispinor and satisfies the Dirac equation (see §7 in Ref. 162, for example). The wave function $\Psi(\mathbf{r}, t)$ can be written

$$\Psi(\mathbf{r}, t) = (\gamma^\mu P_\mu + 1)\tilde{\Psi}(\mathbf{r}, t), \tag{4.9}$$

where $P_\mu = -i\frac{\partial}{\partial x_\mu} - eA_\mu$, the ν^μ are the Dirac matrices, $x_\mu = \{t, x, y, z\}$, and A_μ is the 4-potential of the field. The auxiliary function $\tilde{\Psi}(\mathbf{r}, t)$ satisfies the so-called squared Dirac equation (Subsection 7.4 in Ref. 162). In the laboratory frame of reference, only the scalar potential is nonzero, and the equation for $\tilde{\Psi}$ takes the form

$$\left[\left(i\frac{\partial}{\partial t} - U\right)^2 + \Delta - 1 + i\boldsymbol{\alpha}\nabla U\right]\Psi(\mathbf{r}, t) = 0, \tag{4.10}$$

where $\boldsymbol{\alpha} = \gamma_0\gamma$, Δ is the Laplacian, and U is the potential energy of the particle in the channel.

Equation (4.10) can be simplified substantially for the case at hand, First, as mentioned earlier, the total energy of the relativistic particles, E, is much higher than the potential energy of their interaction with the crystal. The terms U^2 and $\alpha\nabla U$ in (4.10) can thus be ignored. The latter is a measure of the interaction of the spin of the particle with the field of the channel and is less than or comparable to U^2 in order of magnitude. These simplifications correspond to the familiar Furry approximation in relativistic quantum dynamics. Furthermore, the longitudinal and transverse motions of a channeled particle can be separated to some extent. For planar channeling, for example, the wave function $\tilde{\Psi}(\mathbf{r}, t)$ is

$$\tilde{\Psi}(\mathbf{r}, t) = e^{-iEt}e^{i\mathbf{p}_\parallel\boldsymbol{\rho}}\psi(x; E_\parallel), \tag{4.11}$$

where $\mathbf{p}_\parallel$ is the component of the particle momentum parallel to the channeling planes, ρ is a radius vector lying in the channeling plane, and $E = E_\parallel + \varepsilon$ is the total energy of the particle, which we write as the sum of the longitudinal energy, $E_\parallel = \sqrt{p_\parallel^2 + 1}$, and the transverse energy ε. The transverse energy takes on discrete values during channeling and depends parametrically on the longitudinal energy. It is not difficult to show that, under these approximations ($\varepsilon \ll E_\parallel$), the transverse-motion wave functions and the corresponding transverse energies are determined by an equation of the Schrödinger type:

$$\left[-\frac{1}{2E_\parallel}\frac{d^2}{dx^2} + U(x)\right]\psi(x; E_\parallel) = \varepsilon(E_\parallel)\psi(x; E_\parallel). \tag{4.12}$$

A similar two-dimensional equation can be derived for the transverse-motion wave functions in the case of axial channeling.

Within terms $\sim\varepsilon/E$ the quantum equation for the transverse motion is thus nonrelativistic, in complete accordance with the classical equation, (4.6). The longitudinal motion of a channeled particle is described by a plane wave [see (4.11)]. The coupling of the longitudinal and transverse motions in the quantum approach can be seen (first) in a parametric dependence of the distance between transverse-energy levels on the longitudinal energy $E_\parallel \approx E$, which corresponds to an E dependence of the frequency of the classical transverse oscillations. Second, the coupling can be seen in the fact that the wave functions of the transverse motion depend on the longitudinal energy. The wave functions $\psi_n(x; E_\parallel^i)$ and the energy levels $\varepsilon_n(E_\parallel^{-i})$ are thus generally different from the corresponding wave functions $\psi_n(x; E_\parallel^f)$ and energy levels $\varepsilon_n(E_\parallel^f)$. The difference is important only at sufficiently high particle energies, $E \gtrsim 1/\varepsilon$, and it gives rise to several effects in research on channeled particles.[115-119] In the classical approach, these effects correspond to the incorporation of longitudinal oscillations of the particle.

The spin structure of the wave function $\Psi(\mathbf{r}, t)$, determined by the operator $\gamma^{\mu}P_{\mu}+1$ [see (4.9)], is important only for a consideration of the emission of hard photons, with energies $\omega \sim E$. In this case it becomes necessary to take into account the interaction of the particle spin with the effective radiation field.[115] Channeled particles whose energies are not too high ($\lesssim$10–100 GeV), however, emit primarily rather soft photons ($\omega \ll E$). In analyzing the emission spectrum in this frequency range we can completely ignore the spin effects, and we can describe the state of the particles by the scalar wave function[92] $\Psi(\mathbf{r}, t) \approx \tilde{\Psi}(\mathbf{r}, t)$.

For planar channeling, the number of levels (N) in the transverse-motion potential well is determined in order of magnitude by the ratio of the width of the well to the de Broglie wavelength $\lambda_B = \hbar c/\sqrt{2EU_0}$ corresponding to the motion of a particle with a relativistic mass E/c^2 and a kinetic energy of the order of U_0.

When the number of levels in the transverse-motion well becomes large enough, the motion of the channeled particles can be treated by classical mechanics. The discrete nature of the transverse energy can be seen in the emission spectra, however, even if there are many levels, and the condition for the applicability of the classical description of the transverse motion requires a special analysis.

d) Transverse-energy distribution of the particles

An initial transverse-energy distribution of the channeled particles is formed as the particles enter the crystal. Let us assume that a particle is initially moving at an angle $\theta_0 = p_x c/E$ with respect to a crystallographic plane. The probability for the capture of the particle into the level P_i is then determined by the corresponding coefficient in the expansion of a plane wave in terms of the transverse-motion wave functions, as was shown, for example, by Kagan and Kononets[163]:

$$P_i(p_x) \propto |\tilde{\psi}_i(p_x)|^2, \quad \tilde{\psi}_i(p_x) \equiv \int_{-\infty}^{\infty} \exp\left(i\frac{p_x x}{\hbar}\right)\psi_i(x)\,dx. \quad (4.13)$$

The correlation between the phases of different coefficients $\tilde{\psi}_m$ and $\tilde{\psi}_n$, which are wave functions in the momentum representation, is important at distances $l_{mn} \sim 2\pi c/\omega_{mn}$ from the boundary of the crystal $\hbar\omega_{mn} = \varepsilon_n - \varepsilon_m$). The transverse-motion state $|i\rangle$ is thus formed completely over a distance $l \sim 2\pi c/\omega_{i,i-1}$. This distance corresponds to roughly one period of the classical oscillations of the particle in the channel.

In the classical approach, the transverse energy of the particle as it enters the crystal is determined by[93]

$$\varepsilon = \frac{E\theta_0^2}{2} + U(x_0), \quad (4.14)$$

where x_0 is the coordinate of the entry point.

If the entrance angle θ_0 is larger than the critical Lindhard angle $\theta_L = \sqrt{2U_0/E}$, then all the particles lie above the barrier U_0 separating adjacent channels, according to (4.14), and at $\theta_0 = 0$ all the particles enter the channel, except for a small fraction (a few percent) which are incident on the region of thermal vibrations of the atoms.

The coordinate x_0 is a random quantity, distributed equiprobably in the channel. Ryabov[164] has analyzed the transition from the quantum distribution in (4.13) to the classical distribution in (4.14), making use of the semiclassical wave functions in (4.13).

Expressions analogous to (4.13) and (4.14) hold in the case of axial channeling.

Specific calculations of the relative probabilities in (4.13) for the capture of positrons into planar-channeling states for the parabolic potential in (4.1) can be found in the papers by Kumakhov and Wedell[106] and Zhevago.[115] Corresponding calculations for electrons and for a Pöschl-Teller potential, (4.2), have been carried out by Bazylev *et al.*[119,122] Tamura and Kawamura[160] have reported some particular results for axial channeling in a potential like that in (4.3).

As the particles move into the interior of the crystal, their transverse-energy distribution changes. The redistribution is caused by the scattering of the channeled particles by electrons of the crystal, by atoms whose thermal vibrations have taken them away from their equilibrium positions, and by the impurity atoms and dislocations which are unavoiably present in real crystals.

Bazylev and Goloviznin[212] have derived a quantum dynamic theory for the elementary events in which electrons and positrons are scattered during channeling, and they have also derived a theory for the broadening of the transverse-motion levels during channeling. A kinetic theory of the transverse-energy distribution of heavy and light particles has been derived by Beloshitskiĭ and Kumakhov[167,213] on the basis of the Fokker-Planck equations[166] for planar and axial channeling in a classical approach; Kagan and Kononets[163] and also Ryabov[164] have done the same by the quantum approach (for ions and for planar channeling). The dechanneling of ions was examined in detail in a review by Kumakhov.[168] An analysis of the problem of the dechanneling of light particles goes beyond the scope of the present review and requires a special discussion; here we will simply note that the typical thicknesses of various crystals at which channeling is still quite apparent experimentally are given for various electron and positron energies, for planar and axial channels, in Refs. 151, 158–160, and 170–190.

As a particle leaves a crystal, there is an inverse change in the structure of the localized transverse-motion wave functions to a superposition of plane waves with various momentum directions. This structural change occurs over the same scale distances as that during the entrance into the crystal. If the particle leaving the crystal is in the state $\psi_n(x; E)$ the transverse-momentum (or exit-angle) distribution is determined by an expression analogous to (4.13). This distribution has maxima at exit angles corresponding to the quantum-mechanical expectation value of the transverse momentum in the state $\psi_n(x; E)$.

When the number of levels is small, the maxima corresponding to the various bound states can be seen clearly in experiments on the angular distribution of the

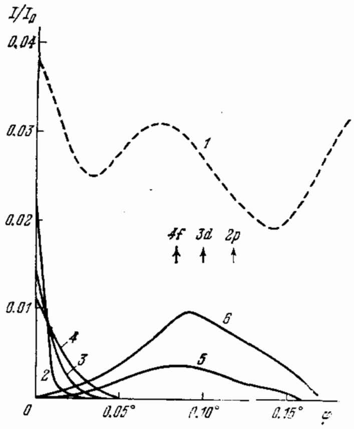

FIG. 11. Angular distribution of the 15-MeV electrons which have passed through a silicon crystal 1.4 μm thick under axial-channeling conditions. 1—Experimental results of Ref. 181; 2–6—results of a model-based calculation of the contributions of various transverse-motion states to the angular distribution.[174]

particles transmitted through a crystal under channeling conditions[159,160,170-176] (Fig. 11). From the behavior of the relative heights of these maxima as a function of the crystal thickness one can estimate the lifetime of the various states.

e) Effects of various factors on the characteristic emission frequencies

From the quantum standpoint, as mentioned earlier, the radiation from channeled particles results from spontaneous transitions between transverse-motion levels.

The dependence of the characteristic emission frequencies on the particle energy and on the nature of the channel potential can be found from simple considerations.[117,118] We begin with energy and momentum conservation during the emission:

$$\begin{gathered} E_i^{\parallel} - E_f^{\parallel} + \varepsilon_i(E_i^{\parallel}) - \varepsilon_f(E_f^{\parallel}) = \hbar\omega, \\ \mathbf{p}_i^{\parallel} - \mathbf{p}_f^{\parallel} = \mathbf{k}^{\parallel}, \end{gathered} \tag{4.15}$$

where the subscript "i" specifies the initial state of the channeled particle, "f" specifies the final state, and $\hbar\omega$ and $\mathbf{k}^{\parallel}$ are respectively the energy and longitudinal momentum of the emitted photon. Assuming that the energy of the photon is small in comparison with that of the particle ($\hbar\omega \ll E$), we can use the approximations

$$\begin{gathered} E_i^{\parallel} - E_f^{\parallel} \approx (\mathbf{p}_i^{\parallel} - \mathbf{p}^{\parallel}_f)\frac{\partial E_i^{\parallel}}{\partial \mathbf{p}_i^{\parallel}}, \\ \varepsilon_f(E_f^{\parallel}) \approx \varepsilon_f(E_i^{\parallel}) - \hbar\omega\frac{\partial\varepsilon_f(E_i^{\parallel})}{\partial E_i^{\parallel}}. \end{gathered} \tag{4.16}$$

We also note that for ultrarelativistic particles we have $|\partial E^{\parallel}/\partial\mathbf{p}^{\parallel}| \approx c[1-(1/2\gamma^2)]$, and the effective angles (θ) between the photon momentum and the longitudinal velocity of the particle, $\mathbf{v}^{\parallel} = \partial E^{\parallel}/\partial\mathbf{p}^{\parallel}$, are small, so that we have $\cos\theta \approx 1-(\theta^2/2)$. At this point we will not consider the frequency dispersion of the electromagnetic field in the crystal ($k = \hbar\omega/c$). As a result we find the following relationship between the frequency and polar angle of the emission:

$$\omega = \frac{2\tilde{\omega}_{if}(E)}{\theta^2 + \gamma^{-2} - 2(\partial\varepsilon_f/\partial E)}, \tag{4.17}$$

where $\tilde{\omega}_{if}(E) = \varepsilon_i(E) - \varepsilon_f(E)$, and $E = E_i^{\parallel} \approx E_f^{\parallel}$. Using the estimate $|\partial\varepsilon/\partial E| \sim |\varepsilon/E|$ we easily see that the last term in the denominator in (4.17) significantly affects the emission frequency at sufficiently high energies,[111,115-119] $E \gtrsim m^2c^4/\varepsilon$.

Expression (4.17) for the emission frequency is amenable to a simple interpretation:[116,127b] In accordance with (Bohr's) correspondence principle, we write the classical analogs of $\tilde{\omega}_{if}(E)$ and $\partial\varepsilon_f/\partial E$ in the form[127b]

$$\tilde{\omega}_{if}(E) = n\omega_0, \quad \frac{\partial\varepsilon_f}{\partial E} = -\frac{\bar{\varepsilon}_{kin}}{E}, \tag{4.18}$$

where $n = i - f$ is the index of the radiation harmonic, $\omega_0(E)$ is the frequency of the classical oscillations of a particle in the channel, and $\bar{\varepsilon}_{kin}$ is the transverse kinetic energy averaged over the oscillation period. Using (4.18), we can write the denominator in (4.17) in the form[116]

$$\theta^2 + \gamma^{-2} - 2\frac{\partial\varepsilon_f}{\partial E} \approx 2(1 - \bar{v}_{\parallel}\cos\theta),$$

where $\bar{v}_{\parallel}$ is the longitudinal velocity of the particle [see (4.8)] averaged over the period of the transverse oscillations.

The dependence of the numerator in (4.17) on the energy of the particle thus results from the relativistic increase in mass, while the denominator in (4.17) is a consequence of the Doppler effect.

The maximum emission frequency, $\omega_{max}^{(i\to f)}$, in a transition from the transverse-motion level f to the level i (emission in the n-th harmonic, in classical terms) corresponds to the forward direction, $\theta = 0$.

In the classical approximation, (4.18), the following result is found for planar channeling in a parabolic potential[111,116,118,119]:

$$\omega_{max}^{(n)} = n\cdot\frac{2^{5/2}U_0^{1/2}E^{3/2}}{dm^2c^3}\,\frac{1}{1+(\varepsilon E/m^2c^4)}\cdot \quad (0 \leqslant \varepsilon \leqslant U_0). \tag{4.19}$$

For the model planar electron channel in (4.2) we have[118b]

$$\omega_{max}^{(n)} = n\frac{2^{3/2}|\varepsilon|^{1/2}E^{3/2}}{bm^2c^3}\left(1 + \frac{2|\varepsilon|E}{m^2c^4}\sqrt{\frac{U_0}{|\varepsilon|} - 1}\right)^{-1}, \tag{4.20}$$

and for axial electron channeling in the potential in (4.3) we have[118]

$$\omega_{max}^{(n)} = n\frac{2^{5/2}|\varepsilon|^{3/2}E^{3/2}}{\alpha m^2c^3}\,\frac{1}{1+(2|\varepsilon|E/m^2c^4)}; \tag{4.21}$$

here $\varepsilon \approx \varepsilon_i(E) \approx \varepsilon_f(E)$ is the transverse energy of the particle.

The frequency of the classical oscillations of the particles in the channel, $\omega_0(E)$, is proportional to $E^{-1/2}$, regardless of the potential. At moderate energies, therefore, at which the classical description of the transverse motion is valid, but at which the longitudinal-oscillation effect is not yet seen ($E \ll m^2c^4/\varepsilon$), the maximum emission frequency at a fixed harmonic n therefore increases in proportion to[96,97] $E^{3/2}$. At higher energies, $E \gtrsim m^2c^4/\varepsilon$ the frequency $\omega_{\max}^{(n)}$ increases more slowly because of the longitudinal oscillations.[115-119] Finally, at energies E low enough for the quantum nature of the transverse motion to become important, the E dependence of the maximum emission frequency for a transition between levels with fixed quantum numbers is determined by the particular potential (Subsection 4f).

Following the results of Refs. 92 and 112–114, we will now show that at relatively low energies ($\varepsilon E \ll m^2c^4$) the frequency $\omega_{\max}^{(i\to f)}$ can be strongly influenced by effects associated with polarization of the medium. When the polarization is taken into account, the relationship between the energy and momentum of the emitted photon becomes

$$k \approx \frac{\hbar\omega}{c}\left(1-\frac{\omega_p^2}{2\omega^2}\right). \tag{4.22}$$

For simplicity here we are considering the case in which the "plasma" formula is valid for the dielectric permittivity. If we use (4.22) in conservation laws (4.15), we find the following to replace (4.17):

$$\theta^2 = \frac{2\tilde{\omega}_{if}}{\omega} - \gamma^{-2} + \frac{\omega_p^2}{\omega^2}. \tag{4.23}$$

The band of x-ray emission frequencies in a transition from level i to a fixed level f is now determined by the condition that the right side of (4.23) be positive:

$$\gamma^2\left(\tilde{\omega}_{if} - \sqrt{\tilde{\omega}_{if}^2 - \omega_p^2\gamma^{-2}}\right) = \omega_{\min}^{(i\to f)} \leqslant \omega \leqslant \omega_{\max}^{(i\to f)} = \gamma^2\left(\tilde{\omega}_{if} + \sqrt{\tilde{\omega}_{if}^2 - \omega_p^2\gamma^{-2}}\right). \tag{4.24}$$

According to (4.24), the extreme frequencies $\omega_{\max}^{(i\to f)}$ and $\omega_{\min}^{(i\to f)}$ are radiated at a zero angle. For x-ray frequencies, the maximum emission angle is

$$\theta_{\max}^{(i\to f)} = \sqrt{\tilde{\omega}_{if}^2(E)\,\omega_p^{-2} - \gamma^{-2}}. \tag{4.25}$$

A single frequency (for a fixed transition $i\to f$) is radiated at this angle:

$$\omega\left(\theta_{\max}^{(i\to f)}\right) = \frac{\omega_p^2}{\tilde{\omega}_{if}(E)}. \tag{4.26}$$

Corresponding to each fixed emission angle $\theta < \theta_{\max}$ there are two different frequencies in the allowed frequency band.

Solving the equation

$$E_{cr}\,\tilde{\omega}_{if}(E_{cr}) = \omega_p \cdot mc^2,$$

we find a critical particle energy, below which frequencies in the x-ray range cannot be radiated. At an energy slightly above E_{cr} a relatively narrow band of allowed frequencies appears near the frequency $\omega_{cr}(E_{cr}) = \omega_p E_{cr}/mc^2$. At energies $E \gg E_{cr}$ the maximum emission frequency is essentially the same as the frequency $\omega_{\max}^{(i\to f)} = 2\gamma^2\tilde{\omega}_{if}$, derived without consideration of the polarization. The minimum x-ray frequency is

$$\omega_{\min}^{(i\to f)} \approx \frac{\omega_p^2}{2\tilde{\omega}_{if}(E)}. \tag{4.27}$$

This minimum frequency increases with increasing energy, but the maximum frequency increases even faster. The frequency band thus expands with increasing value of the ratio E/E_{cr}.

As a rule, the critical energy E_{cr} is low (~1–2 MeV), so that the polarization can have a significant effect on the maximum frequency $\omega_{\max}$ only at particle energies ≤ 10 MeV. On the other hand, the polarization has an important effect[4)] on the minimum emission frequency in (4.27) even at relatively high energies, [92] $E \gg E_{cr}$.

f) Spectral and angular distributions of the Kumakhov dipole radiation

If the energy of the channeled particles is not too high, $E \ll m^2c^4/\varepsilon$, expressions for the spectral and angular densities of the radiation can be derived comparatively simply.[118] For this purpose we will use an auxiliary coordinate system S', which is moving with the particle along the crystal axes or planes at a velocity $v_\parallel$. In this coordinate system, the potential of the channel, U', is $\gamma = [1-(v_\parallel^2/c^2)]^{-1/2}$ times that in the laboratory system.

Let us examine the case of planar channeling in detail. The electric field of the planes forces a particle to oscillate in the S' system at an average transverse velocity $v_\perp' \sim \sqrt{2\varepsilon E}/mc$. In the relativistic case ($\gamma \approx 1$), a magnetic field also arises in S'; this magnetic field is roughly equal to the electric field and is directed along the planes, in the direction perpendicular to the velocity $v_\parallel$. However, if the transverse velocity $v_\perp'$ is nonrelativistic ($v_\perp' \ll c$), the magnetic force exerted on a particle in the S' system is much weaker than the electric force. Consequently, as mentioned earlier, the longitudinal oscillations may be ignored at energies $E \ll m^2c^4/\varepsilon$. Furthermore, the radiation is dipole radiation, since at nonrelativistic velocities $v_\perp'$ the retardation of the radiation field in the region in which the particle is moving can also be ignored. As a result, from the familiar expression for the radiation by a dipole at rest[81] we find the following expression for the spectral-angular power density of the radiation for a transition between levels i and f, after performing a Lorentz transformation[118]:

$$\frac{d^3W_{if}}{d\omega\, d\Omega\, dt} = \frac{\omega^2\omega_{if}^2\,|d_{if}|^2}{2\pi c^3}\left[\sin^2\varphi + \left(\frac{\cos\theta - \beta_\parallel}{1-\beta_\parallel\cos\theta}\right)^2\cos^2\varphi\right] \times \delta\left[\omega\left(1-\beta_\parallel\cos\theta\right) - \omega_{if}\right], \tag{4.28}$$

where d_{if} is the matrix element of the dipole moment, φ is the azimuthal angle of the emission, $\beta_\parallel = v_\parallel/c$, ω_{if}, and ω_{if} is the transition frequency in the laboratory system.

In the dipole approximation, for planar channeling, the radiation in a given direction is completely plane-polarized. The normal to the channeling planes and the vector momentum of the photon define the polarization plane.[102]

We integrate (4.28) over emission angle and sum over the final transverse-motion state. In the ultrarelativistic limit we then find the following result for the spectral power density of the radiation[92,102]:

[4)] As Gevorgyan and Korkhmazyan have shown,[191] similar polarization effects should be observed in gas-filled undulators.

$$\frac{d^2W}{d\omega\, dt} = \frac{\omega}{c^3} \sum_f \tilde{\omega}_{if}^2 |d_{if}|^2 (1 - 2\Omega_{if} + 2\Omega_{if}^2)\, \eta(1 - \Omega_{if}); \tag{4.29}$$

here $\Omega_{if} = \omega/2\gamma^2\tilde{\omega}_{if}$ is the ratio of the emission frequency to the maximum frequency for the given transition (if polarization is ignored), and $\eta(\xi)$ is the Heaviside unit step function.

In the dipole approximation it is a comparatively simple matter to calculate other characteristics of the radiation also. In particular, the total energy lost by a particle on radiation per unit time is found by integrating (4.29) over frequency:[116]

$$\frac{dE}{dt} = -\frac{dW}{dt} = -\frac{4\gamma^4}{3c^3} \sum_f \tilde{\omega}_{if}^4 |d_{if}|^2. \tag{4.30}$$

The radiative width of a transverse-energy level (the transition probability per unit time) is determined in the laboratory coordinate system by

$$\Gamma^{(i)} = \int_0^\infty \frac{d^2W}{d\omega dt} \frac{d\omega}{\hbar\omega} = \frac{4\gamma^2}{3\hbar c^3} \sum_f \tilde{\omega}_{if}^3 |d_{if}|^2. \tag{4.31}$$

Incorporating the finite width of the transverse-energy levels results in a replacement of the δ-function in (4.28) by the function[120]

$$g(\omega) = \frac{1}{2\pi} \frac{\Gamma}{[\omega(1 - \beta_\parallel \cos\theta) - \tilde{\omega}_{if}]^2 + (\Gamma^2/4)}, \tag{4.32}$$

where Γ is half the sum of the level widths. The behavior of the spectral distribution of the radiation near the extreme frequency ($\omega - 2\gamma^2\tilde{\omega}_{if} \lesssim \Gamma 2\gamma^2$) is described by the function

$$G(\omega) = \frac{1}{2}\left(1 - \frac{2}{\pi} \operatorname{arctg} \frac{\omega - 2\gamma^2\tilde{\omega}_{if}}{2\gamma^2\Gamma}\right) \tag{4.33}$$

instead of a step function [see (4.29)]. From the extent to which the edges of the spectrum are "blurred" we can thus determine the lifetimes of a channeled particle in the various transverse-motion states.

Another possibility for determining level lifetimes is to measure the spectral distribution of the radiation into a comparatively small angular interval, $\Delta(\theta^2) \lesssim \Gamma/\gamma^2\tilde{\omega}_{if}$, around some direction ($\theta = 0$) for example. The Doppler broadening can be ignored in this case, and the spectrum is a Lorentzian curve centered at the point $\omega = \omega_{max}^{(i\to f)}$ with a width $\Delta\omega \sim \Gamma\gamma^2$. Since the angle and frequency of the emission are correlated in the case of channeling, the angular discrimination does not lead to a loss in the spectral energy density of the radiation in the corresponding frequency range, in contrast with the case of bremsstrahlung, for example. At the same time, the positions of the peaks in the emission spectrum determine the structure of the transverse-energy levels and thus the average potential of the crystal planes (or axes).

In the case of axial channeling, the following result can be derived for the spectral-angular distribution of the dipole-radiation energy per unit time:[102,119]

$$\frac{d^3W_{if}}{d\omega\, d\Omega\, dt} = \frac{\omega^2\tilde{\omega}_{if}^2}{2\pi c^3} \{|-d_{if}^{(x)} \sin\varphi + d_{if}^{(y)} \cos\varphi|^2 + \left(\frac{\beta_\parallel - \cos\theta}{1 - \beta_\parallel \cos\theta}\right)^2 |d_{if}^{(x)} \cos\varphi + d_{if}^{(y)} \sin\varphi|^2\}\, \delta(\omega(1 - \beta_\parallel \cos\theta) - \omega_{if}). \tag{4.34}$$

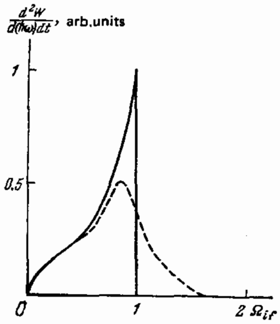

FIG. 12. Typical spectrum of the dipole radiation by a positron in the case of planar channeling. Solid curve—parabolic potential; dashed curve—with anharmonic effects.

The other characteristics of this radiation differ from those for planar channeling [(4.29)–(4.31)] only in that the dipole moment d_{if} is now a two-dimensional vector, in accordance with the nature of the transverse motion during axial channeling.

For the model potentials (4.1)–(4.3), the transition frequencies $\tilde{\omega}_{if}$ and dipole moments d_{if} can be calculated analytically. A particularly simple result is found for planar channeling of positrons in a parabolic potential,[92,97] (4.1):

$$\tilde{\omega}_{if} = \omega_0 (i - f), \quad \omega_0 = \frac{2^{3/2} c}{d} \sqrt{\frac{U_0}{E}}, \; d_{if} = \frac{de}{4} \sqrt{\frac{\varepsilon_i}{U_0}}\, \delta_{i-1,f}. \tag{4.35}$$

In this case the transverse-energy spectrum is equidistant, and dipole radiation can occur only in a transition to the level nearest the initial level. Figure 12 shows the typical shape of the emission spectrum corresponding to (4.29). The peak in the spectral energy density of the radiation occurs at the boundary frequency, which in this case is proportional to $\gamma^{3/2}$. The spectral energy density in the peak increases in proportion to $\gamma^{1/2}$.

For a parabolic potential, the shape of the spectrum is not changed when an average is taken over initial states.

When anharmonic corrections of the type βx^4 to the potential in (4.1) are taken into account,[99b,129] the equidistant spacing of transverse energy levels is disrupted. As a result, after an average is taken over the initial states there is some spreading of the frequency distribution near the boundary frequency, and a fine structure appears at the edge of the emission spectrum. If the deviation from an equidistant arrangement is smaller than the level width, however, this fine structure does not appear, and the spectrum takes the form shown by the dashed curve in Fig. 12. When anharmonic effects are taken into account, transitions to levels further from the initial level and emission at harder frequencies also become possible. The intensity of the emission in this region, however, is comparatively low.

For planar channeling of electrons in potential (4.2) the transverse-energy spectrum is very nonequidistant. The transition frequencies are given by[119]

$$\tilde{\omega}_{if} = \frac{\hbar c^2}{2b^2 E} [2s(E) - i - f](i - f), \quad s(E) = -\frac{1}{2} + \left(\frac{1}{4} + \frac{2b^2 E U_0}{\hbar^2 c^2}\right)^{1/2},$$

where i and f are the quantum numbers of the levels, which take on integer values from zero up to the greatest integer in the parameter $s(E)$. Since the potential is symmetric with respect to the channeling plane, the transverse-motion states have a definite spatial parity. Dipole transitions can occur between states with different parities (the produce $i \cdot f$ must be odd). The matrix elements of the dipole moment for this case were calculated in Ref. 122.

The spectrum of the radiation from channeled electrons, integrated over angle, consists of several bands (like that shown in Fig. 2) with various heights. The various bands correspond to transitions between various levels. These bands overlap only partially. The number of peaks in the spectrum and their positions depend on the number of levels in the potential well in (4.2), and this number is determined by the total electron energy.[92] The relative heights of the peaks depend both on the dipole moments and the populations of the initial levels; the highest peaks correspond to transitions to adjacent levels.

A corresponding picture should be seen for the emission spectrum in the case of axial channeling. The transverse energy in potential (4.3) is quantized in accordance with

$$\varepsilon_{Nl} = -\frac{E\alpha^2}{2\hbar^2c^2}\,\frac{1}{[N-(1/2)]^2},$$

where $N = n + |l| + 1/2, n = 0, 1, 2, \ldots$ is the radial quantum number; and $l = 0, \pm 1, \pm 2, \ldots$ is the projection of the angular momentum of the electron onto the axis (in units of $\hbar$).

Dipole transitions can occur only if there is a unit change in the projection of the angular momentum (with a change in parity). The degeneracy of states in terms of angular-momentum projection must also be taken into account. The matrix elements of the dipole moment can be calculated analytically by an approach similar to that taken for the hydrogen atom.[192,193] For transitions to the 1s ($n = 0, l = 0$), for example, we find $|\mathrm{d}_{if}| = e(\hbar c)^2 c_{if}/\alpha E$, $c_{2p,1s} = 0,24$, and $c_{3p,1s} = 0,1$.

Experiments on channeled electrons and positrons with relatively low energies, at which the quantum nature of the transverse motion is quite apparent, have now been carried out at Stanford,[145,146] Aarhus (Denmark),[149] Albany,[150] Saclay,[211] and Urbana.[214]

The spectral distribution of the radiation from positrons at 56 and 50 MeV has been measured by Alguard *et al.*[145] in the case of planar channeling in a silicon crystal 18 μm thick. They detected the x rays with a germanium detector 9 mm^2 in area and 7 mm thick. The angular divergence of the positron beam was $\Delta\theta \approx 10^{-3}$ rad, comparable to the critical channeling angle $\theta_L \approx 1.5 \times 10^{-3}$. Figure 14 shows a representative spectrum for the case in which the beam is oriented parallel to the (110) planes. The peak at $\hbar\omega \approx 42.5$ is emission from positrons captured into planar channeling. The position of this peak and the nature of the spectrum near the peak agree with theoretical predictions based on model potential (4.1) with the anharmonic correc-

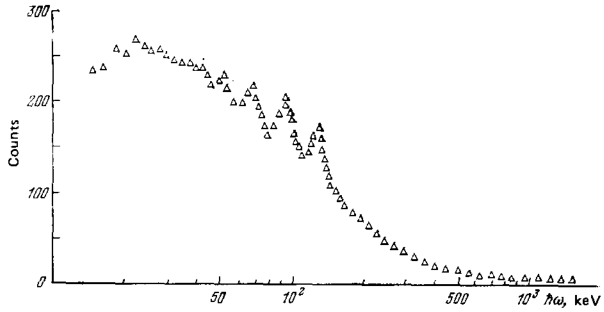

FIG. 13. Spectral distribution of the radiation from electrons with $E = 56$ MeV in silicon with the electron beam parallel to (110) planes.[146]

tions.[129] As the positron energy is reduced to 50 MeV, the peak shifts toward lower frequencies, $\hbar\omega \approx 36.5$ keV, in accordance with the theoretical dependence $\omega_{\mathrm{max}} \propto \gamma^{3/2}$ for planar channeling of positrons. When the crystal planes are rotated with respect to the beam through an angle much larger than the critical channeling angle, $\theta_L = 1.5 \cdot 10^{-3}$, the peak in the emission spectrum disappears. The ratio of the spectral energy density of the radiation in the peak at the frequency $\hbar\omega = 42.5$ keV to the corresponding value for the disoriented target is 2.6.

Since the angular divergence of the particle beam was insufficiently small, and since the length of the crystal was comparable to the dechanneling length, a substantial fraction of the particles moved outside the channels. Accordingly, the peak in the spectrum was seen against a background of emission from above-barrier particles (see Subsection 4h).

The same experimental team measured the emission spectra of electrons at 28 and 56 MeV during planar channeling in silicon.[146]

In contrast with the corresponding experiments with positrons, when the crystal planes were oriented parallel to the electron beam the emission spectra had several peaks, whose number and positions depended on the electron energy. Figure 13 shows this type of spectrum for the case of silicon (110) planes.

Figure 15 shows the potential of the silicon (110) plane [see (4.2)]. The horizontal solid lines are the transverse-energy levels of an electron with a total energy of 56 MeV, and the dashed horizontal lines show the corresponding levels for 28 MeV. The arrows show possible dipole transitions. More-accurate calculations of the positions of the peaks in the emission spectra, based on a numerical solution of the Schrödinger equation, yield the results shown in Table IV (Ref. 215). The agreement of the theoretical values of $\hbar\omega_{if}^{(\mathrm{max})} = 2\gamma^2\hbar\omega_{if}$ with the experimental values is quite good. The shape of the experimental spectra near the peaks is in better agreement with the theoretical predictions incorporating the level width [see (4.33)].

Some measurements at Saclay of the emission spectra of electrons with $E = 54$ MeV in the case of planar channeling in a diamond crystal 20 μm thick were re-

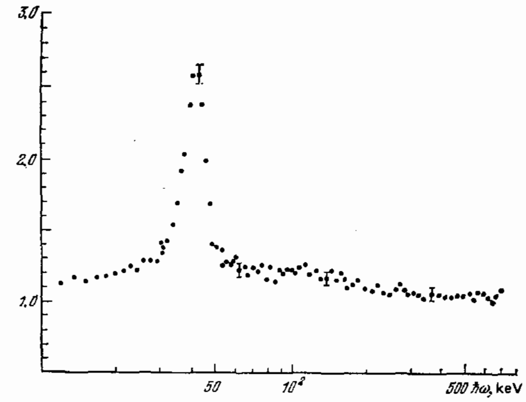

FIG. 14. Spectral distribution of the radiation from positrons with $E = 56$ MeV in a silicon crystal 18 μm thick.[145] The angular divergence of the positron beam is $\Delta\theta = 10^{-3}$; the critical angle for channeling is $\theta_L = 1.5\cdot 10^{-3}$. The positron beam is oriented parallel to (110) planes. The quantity plotted along the ordinate is the ratio of the number of detector counts for the parallel orientation to the corresponding number for a disoriented target.

cently reported.[211] An electron beam with an angular spread of 10^{-4} rad was oriented parallel to the (111), (110), and (100) planes. Figure 16 shows the measured spectral-angular density of the number of photons emitted in the "forward" direction ($\theta = 0$) into a solid angle of $4.3\cdot 10^{-6}$ sr. The number and positions of the peaks in the spectra agree well with the calculations. Since the angular resolution and thus the energy resolution of the photon detector was smaller than the measured line widths, these widths are a consequence of the finite lifetime of the levels and also of multiple scattering of the particle beam parallel to the channeling planes.

Andersen and Laegsgaard[149] have observed emission in the case of channeling of electrons with energies from 1.5 to 4 MeV along the ⟨111⟩ axes in a target 1.2 μm thick. The electron beam had an angular divergence $\leq 0.05°$, much smaller than the critical channeling angle. The lifetime of the axial-channeling 1s state was determined from the width of the line in the spectrum corresponding to the $2p \to 1s$ transition.

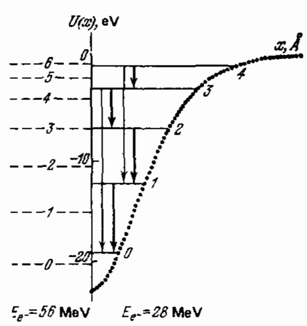

FIG. 15. Potential of a plane for the silicon (110) channel and scheme of transverse-energy levels of electrons with a total energy $E = 28$ MeV (solid lines) or $E \approx 56$ MeV (dashed lines).[122] The arrows show (for 28 MeV) possible dipole radiative transitions; the heavy arrows show the most intense transitions.

TABLE IV. Theoretical[215] and experimental[146] values of the photon energy at the maxima in the spectra radiated by electrons channeled by silicon (110) planes (shown in parenthesis beside the theoretical values are the initial and final quantum numbers, $i \to f$).

$E = 28$ MeV		$E = 56$ MeV	
$\hbar\omega_{if}^{(max)}$ (expt), keV	$\hbar\omega_{if}^{(max)}$ (theo), keV	$\hbar\omega_{if}^{(max)}$ (expt), keV	$\hbar\omega_{if}^{(max)}$ (theo), keV
40	44.8 (1→0)	128	139.1 (1→0)
25	28.9 (2→1)	94	101.4 (2→1)
16	19.8 (3→2)	68	75.4 (3→2)
		52	58.2 (4→3)
		—	45.4 (5→4)

Some analogous measurements of the emission spectra of electrons with energies from 2.0 to 4.5 MeV in a silicon single crystal with a thickness of 4400 Å, oriented with the ⟨110⟩ axis along the beam, have been

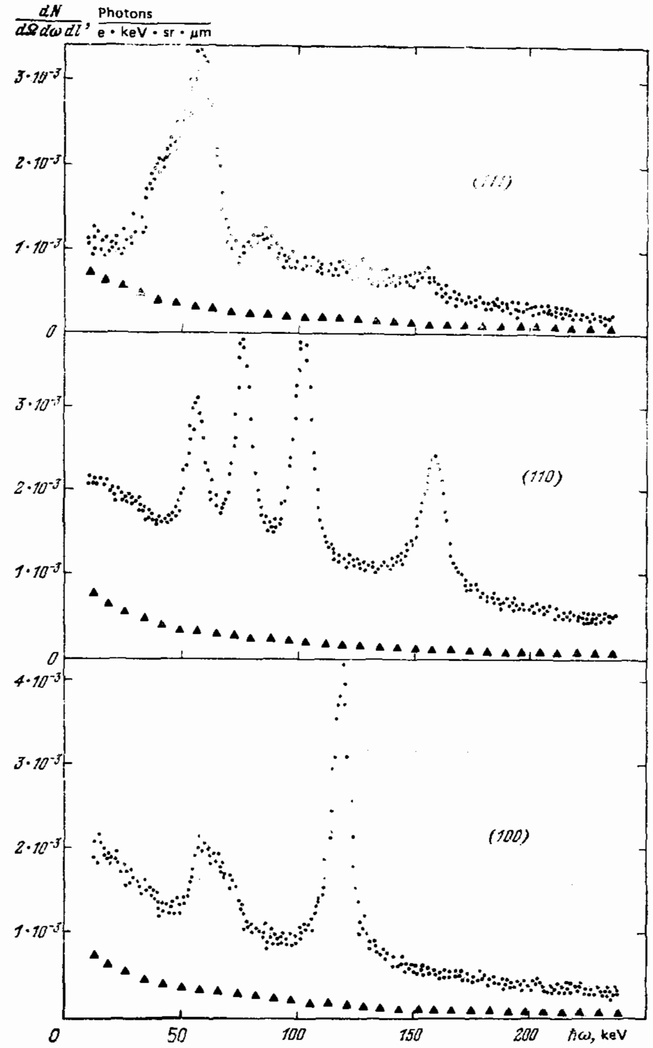

FIG. 16. Spectral-angular density of the number of photons emitted by 54-MeV electrons along the beam direction in the case of channeling along the (111), (110), and (100) planes of a diamond crystal 20 μm thick.[211] ▲—Emission spectrum for a disoriented crystal.

carried out at Albany.[150] The beam had an angular divergence $\sim 1.5 \cdot 10^{-3}$ rad. The positions of the observed spectral peaks agreed with the corresponding theoretical predictions based on the transverse-energy levels of channeled electrons in the field of this axis and also in agreement with measurements carried out at Aarhus.[149]

g) Dipole radiation accompanying classical motion

There is a certain range of channeled-particle energies in which the condition for dipole radiation, $\varepsilon E \ll m^2c^4$, still holds but in which the transverse motion of the particles can be treated classically. As mentioned in Subsection 4c, the conditions for the existence of a sufficiently large number of transverse-energy levels may be insufficient to allow the classical approach in analyzing the emission spectra. Another requirement is that the deviation from an equidistant level arrangement must be much smaller than the level width. In this case the discrete nature of the transverse energy can be completely ignored. During planar channeling of electrons, however, the discrete nature of the transverse-energy spectrum can be significant at energies up to ~1 GeV, where the number of levels reaches 10–20.

According to the correspondence principle, general expressions for the spectral-angular distribution of the dipole radiation can be found for the classical case by replacing the matrix elements of the dipole momentum in (4.28) and (4.34) by the Fourier components of the transverse coordinate and by replacing the sum over the harmonics ($n = 1, 2, \ldots$):

$$x_{if} \to \frac{1}{T}\int_0^T x(t)\, e^{in\omega_0 t}\, \mathrm{d}t, \quad \sum_f \to \sum_n, \quad \tilde{\omega}_{if} \to n\omega_0.$$

As a result, the spectral distribution in (4.29) becomes

$$\frac{\mathrm{d}^2W}{\mathrm{d}\omega\,\mathrm{d}t} = \frac{\omega\omega_0^2}{c^3}\sum_n n^2 |d_n|^2 (1 - 2\Omega_n + 2\Omega_n^2)\, \eta\,(1 - \Omega_n), \tag{4.36}$$

where $\omega_0(E)$ is the frequency of the classical transverse oscillations, $T = 2\pi c/\omega_0$ is the oscillation period, and $\Omega_n = \omega/2\gamma^2 n\omega_0$. Analogous substitutions are made in the case of axial channeling under the condition that the transverse motion is periodic.[119]

As mentioned earlier, the maximum frequency of the dipole radiation at a fixed harmonic is proportional to $\gamma^{3/2}$ in the classical limit, regardless of the potential. The spectral energy density of the radiation at the maximum of a fixed harmonic increases in proportion to $\gamma^{1/2}$.

h) Radiation by above-barrier particles; relationship between the radiation accompanying channeling and coherent bremsstrahlung

As a result of dechanneling or from their very entrance into the crystal (at entrance angles $\theta_0 \neq 0$), some of the particles may have a transverse energy slightly higher than the potential barrier separating adjacent channels [see (4.14)]. The approximation of an average potential is accurate enough to describe the motion of such quasichanneled particles. At the same time, the nature of their motion is quite different from that in a channel and from that in an amorphous medium (or highly disoriented crystal). The spectral and angular distributions of the radiation from above-barrier particles are thus generally different from the corresponding properties in the case of channeling and also different from the properties of ordinary bremsstrahlung.

Simple expressions for the characteristics of the radiation by both channeled and above-barrier electrons and positrons can be derived in the classical dipole approximation.[131,132,134-136,188,111] As above-barrier particles move through the continuous potential of the planes, they radiate as a result of successive collisions with various planes having the same Miller indices. The path traced out by such a particle is a periodic curve. The period T_{ab} is equal to the transit time between adjacent planes. The expression for the radiation spectrum is of the same form as that for the channeled particles, (4.36), but the characteristic frequencies and intensities are generally different. Also different is the importance of inelastic scattering processes which cause changes in the transverse energy.

Curve 1 in Fig. 17 shows the dependence of the positron oscillation frequency ω_0 on the transverse energy ε for a periodic potential which is the parabola of (4.1) between adjacent planes. Also shown here, by curve 2, is the corresponding dependence for electrons for which the potential energy is an "inverted parabola,"

$$U(x) = \frac{4U_0}{d^2}\left(x - \frac{d}{2}\right)^2, \tag{4.37}$$

between adjacent planes. The spectral energy density of the radiation per unit length along the path of the particle can be described by a common expression for particles of different charge and of different transverse energy[133b,135,118]:

$$\frac{\mathrm{d}^2W}{\mathrm{d}\hbar\omega\,\mathrm{d}l} = I_0 \sum_{n=1}^{\infty} n^3 f^2 F_n^2 \Omega_n \left[1 - \frac{2\Omega_n}{f} + 2\left(\frac{\Omega_n}{f}\right)^2\right] \eta\left(1 - \frac{\Omega_n}{f}\right), \tag{4.38}$$

where

$$I_0 = \frac{2^{1/2}e^2\gamma^2}{\hbar c d}\left(\frac{U_0}{E}\right)^{3/2}, \quad \Omega_n = \frac{\omega d m^2 c^4}{c 2^{5/2} E^{3/2} U_0^{1/2} n},$$
$$F_n^{(\mathrm{cp})} = \frac{z}{2}\delta_{n1}, \quad f^{(\mathrm{cp})} = 1 \quad (z < 1),$$
$$F_n^{(\mathrm{ap})} = \frac{\xi^2}{\pi n(\pi^2 n^2 - \xi^2)}, \quad f^{(\mathrm{ap})} = \frac{\pi}{\xi}\,(z > 1),$$

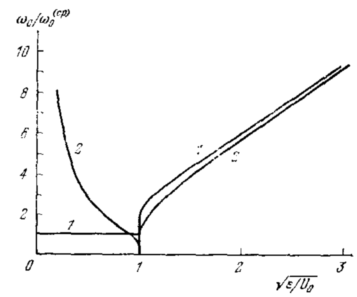

FIG. 17. Frequency of the transverse oscillations of positrons (curve 1) and electrons (2) vs the transverse energy. The oscillation frequency of channeled positrons is assigned a value of unity.

$$\xi = \arcsin z^{-1}, \quad z = \left(\frac{\varepsilon}{U_0}\right)^{1/2},$$

$$F_n^{(\mathrm{ce})} = \frac{2\zeta^2 \delta_{n,\,2l-1}}{\pi n (\pi^2 n^2 + \zeta^2)}, \quad f^{(\mathrm{ce})} = \frac{\pi}{\zeta} \ (z < 1), \quad l = 1, 2, 3, \ldots$$

$$\zeta = 2 \ln(1 + z) - \ln(1 - z^2),$$

$$F^{(\mathrm{ae})} = \frac{\eta^2}{\pi n (\pi^2 n^2 + \eta^2)}, \quad f^{(\mathrm{ae})} = \frac{\pi}{\eta} \ (z > 1),$$

$$\eta = \ln(1 + z) - \frac{1}{2} \ln(z^2 - 1).$$

The superscript (cp) refers to channeled positrons, (ce) to channeled electrons, (ap) to above-barrier positrons, and (ae) to above-barrier electrons.

The positron oscillation frequency undergoes an abrupt change at an energy ε near the barrier height, because of the abrupt change in the nature of the motion as the positrons leave the channeling regime. The oscillation frequencies and thus the characteristic radiation frequencies $\omega_{\max} = 2\gamma^2\omega_0$ of the above-barrier positrons are at least twice as high as those of the channeled positrons. These features are not found in the case of electrons.

With increasing transverse energy of the above-barrier particles, the maximum radiation frequency at a fixed harmonic tends toward $(2\pi c/d)(2\varepsilon/E)^{1/2}$, which corresponds to a nearly rectilinear transverse motion of the particles with a velocity $v_x = c\sqrt{2\varepsilon/E}$. This result does not, of course, depend on the model adopted for the planar potential.

The spectral intensity of the radiation at the maxima in this limit ($\varepsilon \gg U_0$) is proportional to $\sqrt{U_0/\varepsilon}$. With increasing ratio ε/U_0, there is a decrease in the difference in the characteristic radiation frequencies of electrons and positrons. On the other hand, under the condition $\varepsilon \gg U_0$, according to (4.14) we can ignore the effect of the potential of the planes, $U(x_0)$, on the transverse energy as the particles enter the crystal. In this case the transverse energy is determined exclusively by the angle, θ_0, which the particle makes with the plane as it enters the crystal: $\varepsilon \approx E\theta_0^2/2$. At sufficiently large entrance angles $\theta_0 \gg \theta_L$ ($\varepsilon \gg U_0$), therefore, at which the continuous potential of the planes may be treated as a perturbation, we find the familiar results of the theory of coherent bremsstrahlung.[50b] According to these results, the heights of the maxima in the spectra of rather soft radiation ($\hbar\omega \ll E$) are proportional to the angle made by the particle with the crystallographic planes as it enters the crystal, while the frequencies of the maxima are inversely proportional to this angle. If channeling is ignored, these results would remain in force down to very small angles; channeling causes significant deviations from the expected positions for the peaks in the emission spectrum starting at entrance angles θ_0 roughly twice the Lindhard angle. At even smaller angles, $\theta_0 < \theta_L$, the ordinary theory of coherent bremsstrahlung does not give even a qualitatively correct description of the actual dependence of the characteristic radiation frequencies on the particle entrance angle.

We turn now to the shape of the emission spectrum. If we average the spectrum (4.38) over the initial transverse-energy distribution, given by (4.14), we find that the shape of the spectrum depends only on the ratio of

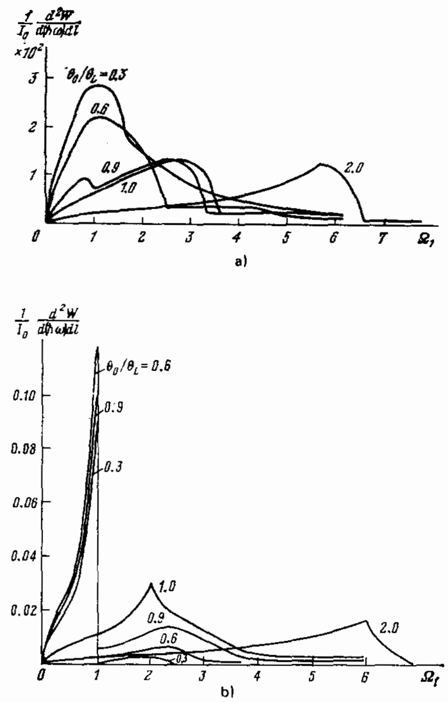

FIG. 18. Spectra of the radiation from positrons and electrons, averaged over the initial transverse-energy distribution, vs the angle at which the particles enter the crystal, θ_0. a—electrons; b—positrons.

the entrance angle θ_0 to the Lindhard angle θ_L. The absolute heights of the peaks in the spectra and their positions in this case depend in a self-preserving manner on the parameters of the potential and on the total particle energy. The situation for the model potential in (4.1) and (4.37) is illustrated by Fig. 18. As the ratio θ_0/θ_L increases, the shape of the spectrum becomes independent of the entrance angle, as expected. The difference between the emission spectra of electrons and positrons fades away. These results correspond to the results of the theory of coherent bremsstrahlung.[50b]

It can be shown[132] in general form, for an arbitrary planar potential, that with increasing θ_0 the expression for the intensity of the dipole radiation by channeled particles transforms into precisely the expression for the intensity of coherent bremsstrahlung in the Born approximation. The corrections to the Born approximation cause a slight difference between the emission spectra of electrons and positrons, as was shown by Akhiezer *et al.* (see Section 7 in Ref. 132) even before a derivation of a systematic theory incorporating channeling. Finally, at entrance angles comparable to, or less than, the Lindhard angle, the emission spectra of electrons and positrons are extremely different—in terms of shape, in terms of the heights of the peaks, and in terms of their positions. Spectra similar to those in Fig. 18 can be found for other model plane potentials.[134-136] It must be kept in mind, however, that when targets with a thickness comparable to the dechanneling length are used the self-preserving dependence of the dipole-radiation spectra disappears, since it becomes necessary to consider a change in the transverse-energy distribution of the particles due to inelastic processes. We also note that if the condition for radiation of a dipole nature is violated the spectral shape after an average is taken over the transverse energy will depend in a more complicated way on the total energy of the particles.[118,127]

In the discussion above we saw the changes in the relationship between coherent bremsstrahlung and the radiation accompanying planar channeling as a function of the angle made by the particles with a crystallographic plane as they enter the crystal. Following Ref. 126, we will now consider this relationship in a different case: in which the angle at which the particles are incident on the plane remains smaller than the Lindhard angle for planar channeling, $\theta_L^{(p)}$, at all times, while the angle made by the particles with the axes lying in this plane can be small enough for coherence effects to occur in the radiation. This case has frequently been discussed in the theory for coherent bremsstrahlung (see Ref. 50b, for example), but channeling has not been taken into account.

In a first approximation, the particle moves along a channeled trajectory under the influence of the continuous potential of the planes. However, since the angle made by the trajectory with the axes is quite small, (but still much larger than the Lindhard angle for axial channeling, $\theta_L^{(a)}$), the particle begins to sense the effects of the individual axes making up the crystallographic plane. In the next approximation in this interaction, the particle trajectory becomes locally curved in various places (in comparison with the wavelength of the oscillation in the planar channel). The effect of the axes occurs in a periodic manner, and the period is determined by the angle between the velocity of the particle and the axes. Formally, the particle is acted upon by the resultant potential $V(x,y)$ of the axes making up the plane; in this case, the potential is conveniently written as a Fourier series,

$$V(x,\ y)=U(x)+\sum_{n=1}^{\infty} U_n(x)\cos\frac{2\pi yn}{d_s},$$

where x is the distance from the plane, and the Oy coordinate axis runs perpendicular to the crystallographic axes. The zeroth term in the expansion of the potential $V(x,y)$ is the continuous potential of the plane; the other terms take into account the discrete nature of the plane along Oy.

The radiation from the particle is the sum of the radiation corresponding to pure planar channeling, discussed above; the radiation accompanying periodic scattering by the atomic axes; and, in general, the result of their interference. However, as a rule, this interference is negligible, since the characteristic frequencies of the channeling radiation are tens of times lower than those of coherent bremsstrahlung in scattering by the individual axes. It may thus be said that the coherent bremsstrahlung exists along with the channeling radiation in this case. However, the channeling, still has an important effect on the coherent bremsstrahlung. The reason is that the channeling causes a redistribution of the impact parameters of the collisions of the particles with the axes in a planar channel (the "flux peaking effect").[168] In particular, during planar channeling the electrons move, on the average, closer to the planes than is usually assumed in the theory for coherent bremsstrahlung without channeling, while the positrons move, on the average, farther from the planes. As a result, the intensities of the coherent bremsstrahlung of electrons and positrons should be significantly different.

The effect of channeling on the coherent bremsstrahlung can be ignored only if the angle at which the particles are incident on the plane is much larger than the Lindhard angle for planar channeling.

In principle, there could also be an emission resulting from radiative transitions from above-barrier states to bound states. Such transitions might be significant at low particle energies, at which there are only a few levels in the well. At high energies, however, the emission of this type is weak in comparison with other types. It is sufficient to say that this type of radiation does not occur at all in the classical approximation.

The semiclassical matrix elements for radiative transitions from above-barrier states to channeling states were calculated in Refs. 127b. The results show that the probability for such transitions contains a small factor e^{-N}, where N is the number of discrete transverse-energy levels. On the other hand, Kalashnikov *et al.*[196-198] found intensities for this type of radiation which were much too high because the calculation method was not appropriate for the problem (the situation is discussed in more detail in Ref. 119).

i) Radiation in the case of axial quasichanneling

Electrons and positrons with transverse energies slightly above the binding energy with an axial channel trace out infinite trajectories in a plane normal to the crystallographic axes. In the approximation of a continuous potential of the axis, the longitudinal motion of these quasichanneled particles has a constant longitudinal momentum [see (4.4)].

In contrast with the planar case, the trajectories of quasichanneled particles are generally not periodic in the axial case. The particles collide with the axes from time to time, and these collisions give rise to a characteristic radiation which differs from both the radiation in the case of channeling and coherent bremsstrahlung.[50b]

Bazylev and Demura[123b] have studied the spectra of the dipole radiation from quasichanneled electrons and positrons at energies low enough to require a quantum-mechanical approach to their scattering.

Avakian *et al.*[123a] have carried out the most detailed analytic calculations of the emission spectra and of the integral radiative loss of high-energy particles during axial quasichanneling. Both classical and quantum-mechanical theories for the effect were derived in these papers.[123] The axis was assigned the potential in (4.3) for specific calculations, and the polarization of the medium was taken into account.

In the classical approach, the trajectories traced out by particles in the transverse plane near one of the axes for this potential are hyperbolas with parameters which depend on the transverse energy of the particle and on the impact parameter of the particle with respect to the axis. The characteristic frequencies and intensities of the radiation accompanying motion along a given trajectory also depend on these parameters. The observed spectrum corresponds to the theoretical spectrum averaged over impact parameter and over transverse energy. The spectral energy density of the radiation in the dipole approximation ($\varepsilon E \ll m^2c^4$) is shown in Fig. 19 as a function of the ratio of the angle at which the particles are incident on the axis to the critical angle $\theta_L = \sqrt{2U_0/E}$, where U_0 is the depth of the real potential well (or the height of the peak, for positrons), used in the calculations as a parameter for cutting off the model potential in (4.3). The average over transverse energy was taken with the initial distribution function, and the subsequent changes in this distribution function as the particles penetrate deeper into the crystal were ignored. The impact parameters of the collisions were assumed to be distributed equiprobably from zero up to half the distance between adjacent axes. In this case the spectra are self-preserving; i.e., when plotted in terms of reduced units of the radiation frequency, the radiation intensity, and the angle of incidence, the spectra are essentially independent of the particular material and axis in the series shown in Table V.

In contrast with the emission spectra in the planar case (Fig. 18), the spectra in Fig. 19 do not have a clearly defined maximum (the abscissa scale is logarithmic). This is a consequence of the random motion of the quasichanneled particles in the transverse plane. The sharp drop in the intensity at reduced frequencies

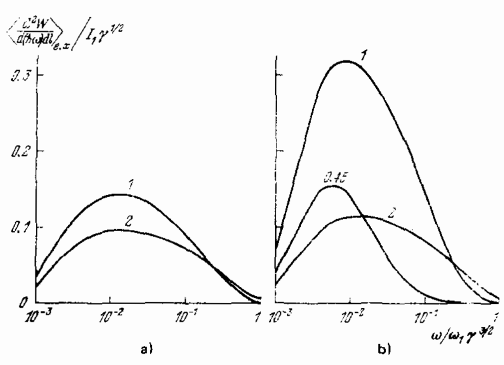

FIG. 19. Energy of the dipole radiation, $d^2W/d(\hbar\omega)dl$, per unit photon energy interval, per unit distance along the path of the particle in a silicon crystal. a—electrons; b—positrons. The quantity plotted along the abscissa is the ratio of the radiation frequency to the frequency $\omega_0\nu^{3/2}$; the quantity plotted along the ordinate is the ratio of $d^2W/d(\hbar\omega)dl$ to the quantity $I_1\nu^{1/2}$ (ν=100). The curves are labeled with the ratio of the angle of incidence of the particle beam on the axis to the critical angle $\theta_L = \sqrt{2U_0/E}$. The spectra for other crystals and for other values of ν are similar to those shown here, in this scale.

TABLE V. Parameters of the spectral characteristics of the radiation from electrons and positrons in the case of axial quasichanneling.

Crystal, axis	$\theta_L\nu^{1/2}$, mrad	$\hbar\tilde{\omega}_0$, eV	I_0, cm^{-1}
Diamond, ⟨110⟩	19.8	1735	0.23
Si, ⟨110⟩	20.9	1609	0.13
Ge, ⟨110⟩	28.0	2208	0.28

$\Omega \gtrsim 1/10$ results from the particular behavior of the continuous potential of the axis (Fig. 10) at relatively small distances, $\rho \lesssim u$. The characteristic frequency Ω in the emission spectrum is proportional to $E^{3/2}$ in the dipole approximation, while the spectral energy density of the radiation is proportional to $E^{1/2}$, as in the case of channeled particles.[96,97] In the general nondipole case, the shape of the emission spectrum remains roughly the same, but the frequencies and intensities of the radiation depend in a different way on the particle energy. In particular, at ultrahigh energies ($\varepsilon E \gg m^2c^4$) the characteristic frequency marking the beginning of the decrease in the radiation intensity is proportional to the square of the particle energy, E^2, while the intensity itself does not depend on E (Ref. 123a).

Yamamura and Ohtsuki[124] carried out a computer simulation of successive collisions of 56-MeV positrons with atoms of ⟨110⟩ axes of a silicon single crystal 2500 Å thick. They found a similar spectral shape for the emission by quasichanneled positrons.

Miroshnichenko *et al.*[143] have measured the emission spectra of positrons in axial quasichanneling at positron energies of 4 GeV; Alguard *et al.*[145] have carried out corresponding measurements at a lower energy, 56 MeV, at which the dipole approximation is valid. The results of Ref. 145 are shown in Fig. 20. The nature of the measured emission is in general agreement with the theory of Refs. 123 and 124. The slight peaks in Fig. 20 can be attributed[145] to positrons which have entered planar channels.

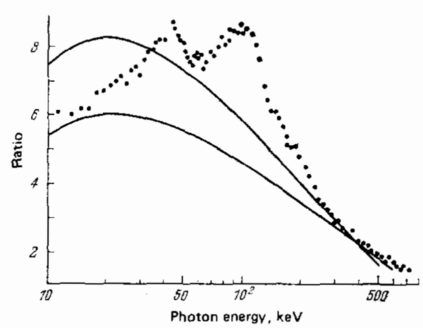

FIG. 20. Ratio of the intensity of the radiation from a 56-MeV positron beam with an angular width of 3 mrad×9 mrad in a silicon crystal 18 μm thick, oriented with its ⟨110⟩ axis along the beam direction, to the corresponding intensity in a disoriented crystal. Points—experimental[145]; curves—calculated.[123] In the calculations the spectra were averaged over the angle of incidence of the positrons within $1.5\theta_L$ (upper curve) and $2\theta_L$ (lower curve).

j) Emission at high channeled-particle energies

According to the results described Subsection 4g, the maximum of the spectral radiation intensity is in the dipole approximation at the first harmonic if longitudinal oscillations of the channeled particles are ignored. The frequency and intensity at the maximum increase with the particle energy E in proportion to $E^{3/2}$ and $E^{1/2}$, respectively. These conclusions, however, break down at high energies, according to the results of Refs. 111, 115–119.

It was shown in Subsection 4e on the basis of elementary considerations that the dependence of the characteristic radiation frequency at a fixed harmonic on the energy of the particle changes substantially when longitudinal oscillations are taken into account. There are also significant changes in the spectral and spectral-angular distributions of the radiation, because a multipole expansion of the radiation field cannot be used at such energies.[92,115,117-119] At high energies ($E \gtrsim m^2c^4U_0^{-1}$), as can be seen easily with the help of (4.21), transitions of a particle from upper levels ($\varepsilon_i \sim U_0$) to the bottom of the well ($\varepsilon_f \approx 0$) also make possible the emission of a photon with an energy $\hbar\omega \sim E$ (Ref. 115). In this case it is necessary to consider the effect of the recoil during the emission on the longitudinal and transverse motion of the channeled particle, and the interaction of the particle spin with the effective radiation field must also be considered.

According to Ref. 115, the spectral-angular distribution of the radiation intensity for the case of planar channeling can be written as follows, where all these effects which arise at high energies are taken into account:

$$\frac{d^3W}{d\omega\, d\Omega\, dt} = \frac{e^2\omega^2}{2\pi c}\sum_f \Big\{\Big(1+u+\frac{u^2}{2}\Big)\big[|I_{if}^{(1)}|^2\theta^2 + |I_{if}^{(2)}|^2 - 2\operatorname{Re} I_{if}^{(1)} I_{if}^{(2)*}\theta\cos\varphi\big] + \frac{u^2}{2\gamma^2}|I_{if}^{(1)}|^2\Big\}\,\delta\Big(\frac{u}{2}\Big[(\theta^2+\gamma^{-2})\frac{E}{\hbar} - \omega\theta^2\cos^2\varphi\Big] - \omega_{if}\Big). \tag{4.39}$$

Here $\hbar\omega_{if} = \varepsilon_i(E) - \varepsilon_f(E-\omega)$, $u = \hbar\omega/(E-\hbar\omega)$, and E is the initial energy of the particle. The matrix elements of the transition current are

$$I_{if}^{(1)} = \int e^{ik_x x}\psi_i^*(x;\ E)\,\psi_f(x;\ E-\hbar\omega)\,dx,$$
$$I_{if}^{(2)} = \frac{i\hbar c}{E}\int e^{ik_x x}\,\frac{d\psi_i^*(x;\ E)}{dx}\,\psi_f(x;\ E-\hbar\omega)\,dx, \tag{4.40}$$

where the transverse-motion wave functions are determined by Eq. (4.12), $k_x = k\theta\cos\varphi$, and $\hbar k$ is the momentum of the photon. The quantities in (4.39) which are proportional to u result from the effect of the recoil on the longitudinal motion of the particle, while the quantities proportional to u^2 result from the interaction of the electron (or the positron) spin with the radiation field. Corresponding results for the axial case were reported in Ref. 123a.

The argument of the δ-function in (4.39) reflects the conservation of energy and longitudinal momentum during the emission, but now—in contrast with (4.17)—the recoil during the emission is taken into account. In particular, an expansion of the type in (4.16) cannot be used in the expression for ω_{if} when the effect of recoil on the transverse motion is taken into account. The effect of the recoil on the longitudinal motion during planar channeling causes the photon energy to become a function of the azimuthal angle. For the soft part of the spectrum ($\hbar\omega \ll E$) we naturally find the earlier expression, (4.17) for the radiation frequency.

The absolute upper boundary of the spectrum, ω_{am}, corresponds to a transition to the bottom of the well ($\varepsilon_f \approx 0$) and to the direction $\theta = 0$. Here

$$\frac{\hbar\omega_{am}}{E} = \frac{2\varepsilon_i E}{m^2c^4 + 2\varepsilon_i E}. \tag{4.41}$$

It follows from (4.41) that, first of all, photons with energies $\hbar\omega \sim E$ can be emitted only by channeled particles of sufficiently high energy, $E \gtrsim m^2c^4/\varepsilon_i$, in the average potential. Second, hard photons with $\hbar\omega \sim E$ are emitted only in transitions with relatively large ($i-f \sim i$) changes in the quantum numbers, for which the difference between the transverse energies is comparable to the energies themselves ($\hbar\omega_{if} \sim \varepsilon_i$).

The transition-current matrix elements in (4.40) can be evaluated analytically for model channel potentials (4.1) and (4.2). The form of these matrix elements and the methods for calculating them are given in Refs. 115, 119 [Eqs. (11) and (16)], and 127b [Eqs. (5) and (6)].

Analysis of the spectral distribution of the radiation found from the general theory leads to the following conclusions. There is a certain optimum energy of the channeled particle, E_{opt}, which depends on the channel potential, at which the spectral power density of the radiation (at the first harmonic) reaches a maximum. Below E_{opt}, the intensity at the first harmonic falls off. Progressively higher harmonics become important, and the spectrum stretches up to higher frequencies. Changes also occur in the angular distribution and the polarization properties of the radiation. For planar channeling, for example, the polarization of the radiation in a given direction transforms from a linear polarization to a generally elliptical polarization.[119]

Miroshnichenko, Avakyan, and others have measured the spectral distribution of the radiation in the case of planar channeling of positrons at 4, 6, 10, and 14 GeV at SLAC.[143] The target was a diamond single crystal, 80 μm thick, oriented with its (110) planes parallel to the positron beam. The optimum energy under these conditions was $E_{opt} = 11$ GeV, so that the influence of the nondipole nature of the radiation and the longitudinal oscillations could be detected. The angular divergence of the beam did not exceed 10^{-5} rad, and the error in the orientation of the crystal was no worse than $1.15\cdot 10^{-5}$ rad. The critical channeling angle $\theta_L = \sqrt{2U_0/E}$ ranged from $1.07\cdot 10^{-4}$ at 4 GeV to $5.7\cdot 10^{-5}$ at 14 GeV according to the calculations of Ref. 127. The photons were detected by a total-absorption NaI(Tl) Cherenkov shower spectrometer with a thickness equal to 20 radiation lengths. The results measured for one spectrum are shown by the points in Fig. 21. The spectral energy density of the radiation emitted by a positron per unit length of the path in the crystal is, at the maximum, 40–60 times the corresponding value for bremsstrahlung in a disoriented crystal.

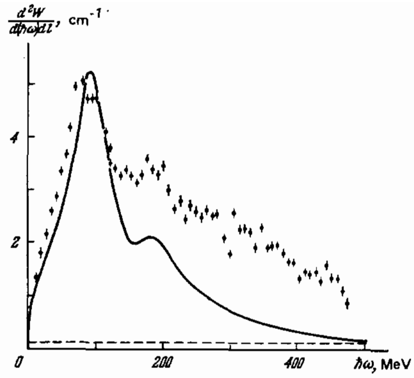

FIG. 21. Spectral energy distribution of the radiation from a positron with an energy of 10 GeV per unit distance along its path in a diamond crystal. The positron beam is oriented parallel to (110) planes. Solid curve—theoretical, with allowance for dechanneling[127b]; dashed curve—ordinary bremsstrahlung in diamond.

There is rather good agreement, especially at 10 and 14 GeV, between the calculated results of Refs. 118, 119, and 127 (Table VI and Fig. 21) and the measurements of the maximum frequency of the first harmonic, $\hbar\omega^{(1)}_{max}$. This agreement is reached only when the longitudinal oscillations are taken into account [the term $\varepsilon E/m^2c^4$ in the denominator in (4.19)].

According to Bazylev *et al.*,[127] the discrepancy which remains between the absolute values of the intensity found experimentally and theoretically can be explained completely by dechanneling of the particles due to imperfections of the crystal (a mosaic nature and dislocations), but the quality of the single crystal was not checked in the experiments, so that more-accurate calculations of the spectra could not be carried out.

Experiments by Miroshnichenko, Avakyan, *et al.*[143] also demonstrated the existence of intense emission in the case of axial channeling of positrons with energies of 4–14 GeV.

The Tsyganov group[142] measured the emission spectra of 10-GeV positrons at Serpukhov as a function of the angle of incidence of the particles on the (110) plane of a silicon crystal. The results of these measurements were quite similar to the corresponding results of Ref. 143 and in generally good agreement with the theory of Ref. 127. In the experiments of Ref. 142, however, an additional peak was found in the spectra, at a frequency equal to roughly half the frequency of the first harmonic of the emission by the channeled particles. This peak has so far remained unexplained.

TABLE VI. Theoretical and experimental values of the maximum photon energy at the first harmonic as a function of the positron energy in the case of channeling by diamond (110) planes.

E, GeV	$\hbar\omega^{(1)}_{max}$ (expt), MeV	$\hbar\omega^{(1)}_{max}$ (theo), MeV
4	23	31
6	42	51
10	90	92
14	120	120

The emission spectra of 4.7-GeV electrons in a diamond single crystal 100 μm thick were measured in the internal beam of the Erevan synchrotron.[144] Agan'yants *et al.*[144] estimated an angular divergence $\approx 2\cdot 10^{-4}$ rad for the electron beam. The photon energy was measured with a double magnetic spectrometer. When the ⟨100⟩ axes and the (110) planes of diamond were oriented parallel to the electron beam (within $4.5\cdot 10^{-5}$ rad), γ rays with energies between ≈20 and 200 MeV were observed to be emitted from the target at an intensity higher than that from a disoriented target. The difference in intensities reached a maximum factor of 80 at a γ energy ≈70 MeV in the axial case and a factor of 30 at a γ energy ≈45 MeV in the planar case.

Similar studies, but at slightly lower electron energies (≈1 GeV) were carried out in the inner beam of the Sirius synchrotron.[148] These experiments also revealed a sharp peak in the spectrum of the photons emitted by channeled electrons in a diamond single crystal 0.35 mm thick oriented with its ⟨110⟩ axis along the beam. This peak corresponded to a photon energy of 20 MeV (at $E = 870$ MeV), and the intensity in the peak exceeded the intensity of the emission from a disoriented target by a factor of about 30.

Some corresponding emission spectra obtained through a computer simulation[124b] of the emission by electrons in a crystal are in approximate agreement with the experimental spectra.[148]

Emission accompanying the axial channeling of 1.2-GeV electrons in a silicon crystal 0.24 mm thick was recently observed on a linear accelerator at Kar'kov.[151] The ratio of the emission intensity to that of bremsstrahlung in an amorphous medium turned out to be 17 over the photon energy range 10–30 MeV, but the peak in the intensity was far less pronounced than in the earlier experiments.[144,148]

k) Analogy with undulator radiation

If external fields are used to force the electron to move along a periodic trajectory, it will radiate electromagnetic waves. If the electron is moving toward the observer at a relativistic velocity, the wavelength of this radiation may be much shorter than the wavelength of the electron oscillation caused by the field. The idea of making use of periodic external magnetic fields to cause charged particles to emit electromagnetic radiation was raised by Ginzburg back in 1947 (Ref. 199). The theory for this type of radiation, which was later named "undulator radiation," was derived by Motz[200] and, especially, some Soviet workers.[201-206] Experimental results have also been obtained, on the undulator radiation by electrons at hundreds of MeV and higher[16-20] over the range from optical frequencies to x-ray frequencies.

The simplest undulator, but still one of considerable practical importance, is one with a magnetic field $H(x)$ which is directed along the Oz axis and whose magnitude varies along the Ox axis sinusoidally[201,202]: $H_z(x)$

$= H\sin(2\pi x/l)$. In such a field, an electron moves along an approximately sinusoidal path. There are also other types of undulators, which make use of the interaction of an electron with spatially periodic magnetic fields of other, more complicated, configurations,[202] and there are also undulators with a constant external field, produced by solenoids and magnetic quadrupole lenses.[202a, 206]

In a broader sense of the term, "undulator radiation" includes the radiation by an electron in an intense external electromagnetic wave,[207-209] coherent bremsstrahlung,[32, 50b] and the radiation accompanying channeling and planar quasichanneling, which was discussed above. In all cases, the motion of the particles can be decomposed, in a first approximation, into a translational motion at a relativistic velocity and an oscillation in the plane perpendicular to the direction of the translational motion.

In many cases the similarities in the motion of the radiating electron can also be seen in some more general properties of the emission spectra. For example, the general classical equations[92, 96, 97, 115, 130] for calculating the radiation spectrum for the planar channeling of high-energy particles differ only in notation from the corresponding equations for the radiation in magnetic undulators.[202c] The same can be said of Eq. (4.36), for the dipole radiation accompanying planar quasichanneling. There is an even closer analogy between the spectrum of the relatively soft radiation accompanying the planar channeling of positrons[92] and the spectrum of the undulator radiation in a plane, harmonic magnetic field.[201, 202]

On the other hand, each of these types of radiation has its own distinctive features, which are related to the particular nature of the field with which the electron interacts. In coherent bremsstrahlung, for example, an important role is played by the thermal vibrations of the lattice atoms, which give rise to an amorphous background in the radiation spectrum.[50b] These effects cannot be taken into account in the undulator approach. The quantum effects associated with the recoil accompanying the emission of a hard photon ($\hbar\omega \sim E$) by an electron in a light wave or in the case of coherent bremsstrahlung are essentially not seen in the case of radiation in deliberately imposed external fields. This difference arises because these external fields generally have a much longer period than the naturally occurring fields or are much weaker. For this reason, the theories for these types of radiations have developed independently.

The radiation emitted by particles in crystals in the cases of channeling and quasichanneling has some distinctive features. First, as shown above, the quantum nature of the transverse motion of the particles is extremely important at sufficiently low energies of the channeled particles. Accordingly, as we have pointed out previously,[92, 121] the radiation by the channeled particles in this case is closer to the radiation of a moving atom, and the analogy with undulator radiation breaks down, since in that case the motion is essentially always classical. The quantum effects in the motion of the electrons can be seen[118, 119] in the radiation spectra up to comparatively high particle energies (1 GeV in the case of planar channeling of electrons).

At high energies, when the transverse motion of the particles can be described in terms of paths, and at relatively soft frequencies ($\hbar\omega \ll E$), the differences from undulator radiation become more formal. For example, the average potential of the planes or axes takes a form characteristic of the given type of channeling, which corresponds to certain paths of the channeled particles. The frequency at which the particles oscillate in the channel depend on the total energy of the particles, in contrast with the case in undulators with an alternating magnetic field. Admittedly, this dependence does occur in quadrupole-lens undulators, but this type of undulator has not received the theoretical or experimental study that the other types have. Since the transverse energy of the channeled particles as they enter the crystal can have any value over a certain range [see (4.14)], an additional average must be taken over the oscillation amplitude in calculating the observable radiation spectra, in contrast with the case of undulators. As a result, the spectra become extremely sensitive to the dynamics of the transport of the particle beam during channeling, i.e., extremely sensitive to a process of any sort which would lead to a further redistribution of the particles in transverse energy.

The radiation accompanying axial quasichanneling is a special case, which has no analog in the theory of undulator radiation, because the transverse motion is aperiodic in this case.

Finally, in the emission of relatively hard photons, with $\hbar\omega \sim E$, by a high-energy channeled particle it is important to consider the effect of the quantum recoil on the transverse motion of the particle, i.e., on the position of the final transverse-energy level $\varepsilon_f(E - \hbar\omega)$ [see (4.39)]. An expansion of the type in (4.15) would not be legitimate at $\hbar\omega \sim E$, so that the energy of the emitted photon cannot be expressed [as it is in (4.17)] in terms of the average longitudinal velocity of the particle [see (4.18)]. In undulators with an alternating magnetic field, the frequency of the transverse oscillations does not depend on the energy; this effect is unimportant; and the recoil affects only the longitudinal motion of the particle. Consequently, there is not a complete analogy between undulator radiation and the radiation accompanying channeling at hard frequencies ($\hbar\omega \sim E$). Results derived recently by Baier *et al.*[137, 210] cannot be applied to the hard radiation accompanying channeling, since these results completely ignore this feature of the emission at hard frequencies.[127b]

In summary, the radiation accompanying channeling and quasichanneling has many properties in common both with undulator radiation and coherent bremsstrahlung. The analogy which holds between these types of radiation in certain cases is of major interest for the development of the theory for these phenomena,[20, 92, 96, 136] but the radiation accompanying channeling is essentially a new type of radiation, which requires further theoretical and experimental research.

[1]R. Tousey, Appl. Opt. **1**, 679 (1962).
[2]A. P. Lukirskii, M. A. Rumsh, and L. A. Smirnov, Opt. Spektrosk. **11**, 505 (1960).
[3]T. M. Zimkina and V. A. Fomichev, Ul'tramyagkaya rentgenovskaya spektroskopiya (Ultrasoft X-Ray Spectroscopy), Izd. Leningr. Univ., Leningrad, 1971.
[4]Y. Farge and P. J. Duke, European Synchrotron Radiation Facility. Supplement 1, Strasbourg: European Science Foundation, 1979.
[5]R. Godvin, Usp. Fiz. Nauk **101**, 697 (1970).
[6]G. P. Hughes and R. C. Fink, Electronics **23**, 99 (1978).
[7]P. Marsh, New Sci. **82**, No. 1157, 712 (1979).
[8]M. A. Mokul'skiĭ, Priroda **3**, 6 (1976).
[9]A. Freund (editor), Proceedings of the International Workshop on the Applications of Intense Capture γ-ray Sources, Nucl. Instrum. Meth. **166**, No. 1 (1979).
[10]B. L. Berman and S. C. Fultz, Rev. Mod. Phys. **47**, 713 (1975).
[11]B. L. Berman (editor), Proceedings of International Conference on Photonuclear Reactions and Applications, Lawrence Livermore Lab., Livermore, 1973.
[12]G. Chapline and L. Wood, Phys. Today **28**(6), 41 (1945) [Russ. Transl. Usp. Fiz. Nauk **121**, 331 (1977)].
[13]U. Knessl, E. A. Koop, G. Kuhl, K. H. Leister, and A. Weller, Nucl. Instrum. Meth. **127**, 1 (1975).
[14]O. F. Kulikov, Tr. FIAN SSSR **80**, 3 (1975); L. Federici, G. Giordano, G. Matone, *et al.*, Nuovo Cimento **B59**, 247 (1980).
[15]G. N. Kulipanov and A. N. Skrinskiĭ, Usp. Fiz. Nauk **122**, 369 (1977) [Sov. Phys. Usp. **20**, 559 (1977)].
[16]H. Winick and E. Spencer, Nucl. Instrum. Meth. **172**, 45 (1980).
[17]CERN Courier **20**, 157 (1980).
[18]A. S. Artamonov, L. B. Barkov, V. B. Baryshev, *et al.*, Nucl. Instrum. Meth. **177**, 239 (1980).
[19]S. Krinsky, IEEE Trans. Nucl. Sci. **NS-26**, 73 (1979); M. Bazin and Y. Farge, IEEE Trans. Nucl. Sci. **NS-26**, 61 (1979).
[20]a) D. F. Alferov, Yu. A. Bashmakov, K. A. Belovintsev, E. G. Bessonov, and P. A. Cherenkov, Pis'ma Zh. Eksp. Teor. Fiz. **26**, 525 (1977) [JETP Lett. **26**, 385 (1977)]; Preprint No. 13, P. N. Lebedev Physics Institute, Academy of Sciences of the USSR, Moscow, 1978; b) A. N. Didenko, A. V. Kozhevnikov, A. F. Medvedev, and M. M. Nikitin, Pis'ma Zh. Tekh. Fiz. **4**, 689 (1978) [Sov. Tech. Phys. Lett. **4**, 277 (1978)].
[21]I. E. Tamm and I. M. Frank, Dokl. Akad. Nauk SSSR **14**, 107 (1937).
[22]V. P. Zrelov, Izluchenie Vavilova–Cherenkova i ego primenenie v fizike vysokikh énergiĭ (Vavilov–Cherenkov Radiation and Its Applications in High-Energy Physics), Atomizdat, Moscow, 1968.
[23]I. M. Frank, in: Problemy teoreticheskoĭ fiziki (Problems of Theoretical Physics), Nauka, Moscow, 1972.
[24]I. E. Tamm, Usp. Fiz. Nauk **68**, 387 (1959); I. M. Frank, Usp. Fiz. Nauk **68**, 397 (1959); P. A. Cherenkov, Usp. Fiz. Nauk **68**, 377 (1959) [Sov. Phys. Usp. **68**, 195 (1959)].
[25]V. L. Ginzburg, Teoreticheskaya fizika i astrofizika (Theoretical Physics and Astrophysics), Nauka, Moscow, 1975.
[26]B. M. Bolotovskiĭ, Usp. Fiz. Nauk **62**, 201 (1957); **75**, 295 (1961).
[27]M. A. Piestrup, R. H. Pantell, H. E. Puthoff, and G. B. Rothbart, J. Appl. Phys. **44**, 5160 (1973).
[28]M. A. Piestrup, R. A. Powell, G. B. Rothbart, C. K. Chen, and R. H. Pantell, Appl. Phys. Lett. **28**, 92 (1976).
[29]V. A. Bazylev, V. I. Glebov, É. I. Denisov, N. K. Zhevago, and A. S. Khlebnikov, Pis'ma Zh. Eksp. Teor. Fiz. **24**, 406 (1976) [JETP Lett. **24**, 371 (1976)].
[30]V. A. Bazylev, V. I. Glebov, É. I. Denisov, N. K. Zhevago, and A. S. Khlebnikov, Preprint IAÉ-2765, I. V. Kurchatov Institute of Atomic Energy, Moscow, 1977.
[31]A. V. Kolpakov, Yad. Fiz. **16**, 1003 (1972) [Sov. J. Nucl. Phys. **16**, 554 (1972)].
[32]M. L. Ter-Mikaelyan, Zh. Eksp. Teor. Fiz. **25**, 296 (1953).
[33]E. L. Feĭnberg, Usp. Fiz. Nauk **132**, 255 (1980) [Sov. Phys. Usp. **132**, 629 (1980)].
[34]V. V. Yakimets, in: Prokhozhdenie izlucheniya cherez veshchestvo (Passage of Radiation Through Matter), Atomizdat, 1968.
[35]V. W. Pafomov, Dokl. Akad. Nauk SSSR **213**, 819 (1973) [Sov. Phys. Dokl. **18**, 229 (1973)].
[36]V. A. Bazylev, A. A. Varfolomeev, and N. K. Zhevago, Zh. Eksp. Teor. Fiz. **66**, 464 (1974) [Sov. Phys. JETP **39**, 222 (1974)].
[37]G. M. Garibyan and G. A. Chalikyan, Zh. Eksp. Teor. Fiz. **35**, 1282 (1958) [Sov. Phys. JETP **6**, 985 (1958)].
[38]G. M. Garibyan, Izv. Akad. Nauk SSSR, Ser. Fiz. **26**, 754 (1962).
[39]J. B. Birks, Rep. Prog. Phys. **38**, 903 (1975).
[40]H. Hönl, Ann. Phys. (Leipzig) **18**, 538 (1933).
[41]V. A. Arakelyan, in: Trudy mezhdunarodnogo simpoziuma po perekhodnomu izlucheniyu chastits vysokikh énergiĭ (Proceedings of the International Symposium on the Transition Radiation of High-Energy Particles), Erevan, 1977, p. 336.
[42]U. Fano and J. W. Cooper, Rev. Mod. Phys. **40**, 441 (1968). (Russ. transl. Nauka, Moscow, 1972).
[43]W. J. Veigele, Atomic Data **5**, 51 (1973).
[44]J. H. Hubbell, Atomic Data **3**, 241 (1971).
[45]U. Bonse and G. Materlik, Z. Phys. **B24**, 189 (1976).
[46]V. A. Bazylev, V. I. Glebov, É. I. Denisov, N. K. Zhevago, A. S. Khlebnikov, V. G. Tsinoev, and Yu. P. Chertov, Pis'ma Zh. Eksp. Teor. Fiz. **34**, 103 (1981) [JETP Lett. **34**, 97 (1981)]; Zh. Eksp. Teor. Fiz. **81**, 1664 (1981) [Sov. Phys. JETP **54**, 884 (1981)].
[47]V. M. Samsonov, Zh. Eksp. Teor. Fiz. **75**, 88 (1978) [Sov. Phys. JETP **75**, 44 (1978)].
[48]V. A. Dzhrbashyan, Izv. Akad. Nauk Arm. SSR, Ser. Fiz. **10**, 427 (1975); **11**, 423 (1976).
[49]V. V. Fedorov and A. I. Smirnov, Pis'ma Zh. Eksp. Teor. Fiz. **23**, 34 (1976) [JETP Lett. **23**, 29 (1976)].
[50]M. L. Ter-Mikaelyan, a) Dokl. Akad. Nauk SSSR **134**, 318 (1960) [Sov. Phys. Dokl. **5**, 1015 (1960)]. b) Vliyanie sredy na élektromagnitnye protsessy pri vysokikh énergiyakh (Effect of the Medium on Electromagnetic Processes at High Energies), Izd. Akad. Nauk. Arm. SSR, Erevan, 1969.
[51]Ya. B. Faĭnberg and I. A. Khizhnyak, Zh. Eksp. Teor. Fiz. **32**, 883 (1957) [Sov. Phys. JETP **5**, 720 (1957)].
[52]G. M. Garibyan, Zh. Eksp. Teor. Fiz. **35**, 1435 (1958) [Sov. Phys. JETP **5**, 720 (1957)].
[53]P. V. Bliokh, Izv. Vyssh. Uchebn. Zaved., Radiofiz. **2**, 63 (1959).
[54]V. E. Pafomov, Zh. Eksp. Teor. Fiz. **39**, 134 (1960) [Sov. Phys. JETP **12**, 97 (1960)].
[55]F. G. Bass and V. M. Yakovanko, Usp. Fiz. Nauk **86**, 189 (1965) [Sov. Phys. Usp. **8**, 420 (1965)].
[56]N. K. Zhevago, Zh. Eksp. Teor. Fiz. **72**, 428 (1977) [Sov. Phys. JETP **45**, 224 (1977)].
[57]G. M. Garibyan, L. A. Gevorgyan, and Yan Shi, Zh. Eksp. Teor. Fiz. **66**, 552 (1974) [Sov. Phys. JETP **39**, 265 (1974)].
[58]G. M. Garibyan and Yan Shi, Izv. Akad. Nauk Arm. SSR, Ser. Fiz. **12**, 105 (1977).
[59]Yan Shi, in: Trudy Mezhdunarodnogo simpoziuma po perekhodnomu izlucheniyu chastits vysokikh énergiĭ (Proceedings of the International Symposium on the Transition Radiation of High-Energy Particles), Erevan, 1977, p. 123.
[60]L. C. L. Yuan, Trudy Mezhdunarodnogo simpoziuma po perekhodnomu izlucheniyu chastits vysokikh énergiĭ (Proceedings of the International Symposium on the Transition Radiation of High-Energy Particles), Erevan, 1977, p. 81.
[61]K. Hoshino, Y. Ohashi, A. Okada, K. Taira, and K. Yokoi, Acta Phys. Acad. Sci. Hung. **29**, Suppl. 4, 443 (1970).
[62]L. C. L. Yuan, C. L. Wang, H. Uto, and S. Prünster, Phys. Lett. **31B**, 603 (1970).
[63]A. I. Alikhanian, K. M. Avakian, G. M. Garibian, M. P. Lorikian, and K. K. Shikhliarov, Phys. Rev. Lett. **25**, 635

(1970).
[64]A. I. Alikhanian, S. A. Kankanian, A. G. Oganesian, and A. G. Tumanian, Phys. Rev. Lett. **30**, 109 (1973).
[65]J. Fischer, S. Iwata, V. Radeka, C. L. Wang, and W. J. Willis, Phys. Lett. **B49**, 393 (1974).
[66]R. Ellsworth, J. MacFall, G. Yodth, F. Harris, T. Katsura, S. Parker, V. Peterson, L. Shiraiski, V. Stenger, J. Mulvey, B. Brooks, and J. Cobb, in: Proceedings of the Thirteenth International Conference on Cosmic Rays, Denver, Col. Assoc. Univ. Press, Boulder, 1973, p. 2819.
[67]M. L. Cherry, Phys. Rev. **D9**, 1112 (1973).
[68]M. L. Cherry, G. Hartmann, D. Müller, and T. A. Prince, Phys. Rev. D10, 3594 (1974).
[69]T. A. Prince, D. Müller, G. Hartmann, and M. L. Cherry, Nucl. Instrum. Meth. **123**, 231 (1975).
[70]L. C. L. Yuan, P. W. Alley, A. Bamberger, and G. F. Dell, Nucl. Instrum. Meth. **127**, 17 (1975).
[71]L. C. L. Yuan, P. W. Alley, G. F. Dell, R. Keller, and H. Uto, Nucl. Instrum. Meth. **130**, 45 (1975).
[72]R. Bosshard, J. Fischer, S. Iwata, V. Radeka, C. L. Wang, and M. Atac, Nucl. Instrum. Meth. **127**, 141 (1975).
[73]C. Camps, V. Commichan, M. Deutschann, H. Gödeke, K. Hangarter, W. Listmann, U. Pützhofen, and R. Schulte, Nucl. Instrum. Meth. **131**, 411 (1975).
[74]C. W. Fabjan and W. Struczinski, Phys. Lett. **B57**, 4836 (1975).
[75]J. Cobb, C. W. Fabjan, S. Iwata, C. Kourkonmelis, A. J. Lankford, G. C. Moneti, A. Nappi, R. Palmer, P. Rehak, W. Struczinski, and W. Willis, Phys. Lett. **B140**, 413 (1977).
[76]C. W. Fabjan, Phys. Lett. **B146**, 343 (1977).
[77]M. L. Cherry and D. Müller, Phys. Rev. Lett. **38**, 5 (1978).
[78]M. L. Cherry, Phys. Rev. **D17**, 2245 (1978).
[79]A. N. Chu, M. A. Piestrup, T. W. Barber, and R. H. Pantell, in: Eighth International Conference on Atomic Collisions in Solids, Abstract, Hamilton, 1979, p. 89.
[80]M. A. Ter-Mikaelyan, Pis'ma Zh. Eksp. Teor. Fiz. **8**, 100 (1968) [JETP Lett. **8**, 61 (1968)].
[81]L. D. Landau and E. M. Lifshitz, Élektrodinamika sploshnykh sred, Gostekhizdat, Moscow, 1957 (Electrodynamics of Continuous Media, Addison-Wesley, Reading, Mass, 1960).
[82]Z. G. Pinsker, Dinamicheskoe rasseyanie rentgenovskikh lucheĭ v ideal'nykh kristallakh (Dynamic X-Ray Scattering in Ideal Crystals), Nauka, Moscow, 1974.
[83]B. W. Batterman and H. Cole, Rev. Mod. Phys. **36**, 681 (1964).
[84]V. A. Belyakov, Pis'ma Zh. Eksp. Teor. Fiz. **13**, 254 (1971) [JETP Lett. **13**, 179 (1971)].
[85]G. M. Garibyan and Yan Shi, Zh. Eksp. Teor. Fiz. **61**, 930 (1971) [Sov. Phys. JETP **34**, 495 (1971)]; **63**, 1198 (1972) [Sov. Phys. JETP **36**, 631 (1972)].
[86]A. L. Avakyan, M. A. Aginyan, G. M. Garibyan, and Yan Shi, Zh. Eksp. Teor. Fiz. **69**, 1049 (1975) [*sic*].
[87]M. Aginyan and Yan Shi, Cited in Ref. 59, p. 193.
[88]A. M. Afanas'ev and M. A. Aginyan, Cited in Ref. 59, p. 169; Zh. Eksp. Teor. Fiz. **74**, 570 (1978) [Sov. Phys. JETP **47**, 300 (1978)].
[89]V. G. Baryshevskiĭ and I. D. Feranchuk, Zh. Eksp. Teor. Fiz. **61**, 944 (1971) [Sov. Phys. JETP **34**, 502 (1971)]; **64**, 760 (1973).
[90]V. G. Baryshevskiĭ and I. D. Feranchuk, Dokl. Akad. Nauk BSSR **18**, 499 (1974).
[91]A. M. Afanasiev and Yu. Kagan, Acta Crystallogr. **A24**, 163 (1968).
[92]V. A. Bazylev and N. K. Zhevago, Zh. Eksp. Teor. Fiz. **73**, 1697 (1977) [Sov. Phys. JETP **46**, 891 (1977)].
[93]J. Lindhard, Danske Vid. Selsk. Mat. Fiz. Medd. **34**, 14 (1965).
[94]D. S. Gemmell, Rev. Mod. Phys. **46**, 129 (1974).
[95]M. Thompson, Contemp. Phys. **9**, 375 (1968); [Russ. transl. Usp. Fiz. Nauk **99**, 297 (1969)].
[96]M. A. Kumakhov, Phys. Lett. **A57**, 17 (1976); Dokl. Akad. Nauk SSSR **230**, 1077 (1976) [Sov. Phys. Dokl. **21**, 581 (1976)].
[97]M. A. Kumakhov, Phys. Status Solidi **b84**, 41 (1977); Zh. Eksp. Teor. Fiz. **72**, 1489 (1977) [Sov. Phys. JETP **45**, 781 (1977)].
[98]A. A. Vorobiev, V. V. Kaplin, and S. A. Vorobiev, Nucl. Instrum. Meth. **127**, 265 (1975).
[99]M. A. Kumakhov and R. Wedell, a) Phys. Lett. **A59**, 403 (1976); b) Phys. Status Solidi **84**, 581 (1977).
[100]V. V. Beloshitsky, M. A. Kumakhov, and R. Wedell, in: Seventh International Conference on Atomic Collisions in Solids, Abstracts of Papers, Moscow, Moscow State Univ. Publ. House, 1977, p. 76.
[101]M. A. Kumakhov, in: Seventh International Conference on Atomic Collisions in Solids, Abstracts of Papers, Moscow, Moscow State Univ. Publ. House, 1977, p. 375.
[102]V. V. Beloshitskiĭ and M. A. Kumakhov, Dokl. Akad. Nauk SSSR **237**, 71 (1977) [Sov. Phys. Dokl; **22**, 645 (1977)]; Zh. Eksp. Teor. Fiz. **74**, 1244 (1978) [Sov. Phys. JETP **47**, 652 (1978)]; Phys. Lett. A69, 247 (1978).
[103]V. V. Beloshitsky, Phys. Lett. **A64**, 95 (1977).
[104]M. A. Kumakhov, Pis'ma Zh. Tekh. Fiz. **3**, 1025 (1977) [Sov. Tech. Phys. Lett. 3, 419 (1977)].
[105]M. A. Kumakhov and R. Vedel', Pis'ma Zh. Tekh. Fiz. **5**, 539 (1979) [Sov. Tech. Phys. Lett. **5**, 220 (1979)].
[106]M. A. Kumakhov and R. Wedell, Phys. Status Solidi **b92**, 65 (1979).
[107]M. A. Kumakhov and R. Vedel', Pis'ma Zh. Tekh. Fiz. **4**, 1411 (1978) [Sov. Tech. Phys. Lett. **4**, 570 (1978)].
[108]M. A. Kumakhov, Usp. Fiz. Nauk **127**, 531 (1979) [Sov. Phys. Usp. **22**, 193 (1979).
[109]R. Wedell, Radiat. Eff. **38**, 165 (1978); Phys. Status Solidi **b87**, 491 (1978).
[110]O. Greschner and R. Wedell, Phys. Status Solidi **b95**, 137 (1979).
[111]M. A. Kumakhov and Ch. G. Trikalinos, Phys. Status Solidi **b99**, 449, (1980); Zh. Eksp. Teor. Fiz. **78**, 1623 (1980) [Sov. Phys. JETP **51**, 815, (1980)].
[112]V. A. Bazylev and N. K. Zhevago, Preprint IAE-2865, I. V. Kurchatov Institute of Atomic Energy, Moscow, 1977.
[113]V. A. Bazylev and N. K. Zhevago, Cited in Ref. 100, p. 65; in: Trudy VII Mezhdunarodnoĭ konferentsii po atomnym stolknoveniyam v tverdykh telakh (Proceedings of the Seventh International Conference on Atomic Collisions in Solids), September 19–23, 1977, Moscow, Izd. Mosk. Univ., Moscow, Vol. 1, p. 132.
[114]V. A. Bazylev and N. K. Zhevago, Phys. Lett. **B84**, 182 (1979).
[115]N. K. Zhevago, Zh. Eksp. Teor. Fiz. **75**, 1389 (1978) [Sov. Phys. JETP **48**, 701 (1978)].
[116]V. A. Bazylev and N. K. Zhevago, Zh. Eksp. Teor. Fiz. **77**, 1267 (1979) [Sov. Phys. JETP **50**, 637 (1979)]; Radiat. Eff. **54**. 221 (1981).
[117]V. A. Bazylev and N. K. Zhevago, Usp. Fiz. Nauk **127**, 529 (1979) [Sov. Phys. Usp. **22**, 191 (1979)].
[118]V. A. Bazylev and N. K. Zhevago, Radiat. Eff. **54**, 41 (1981).
[119]V. A. Bazylev, V. I. Glebov, and N. K. Zhevago, Zh. Eksp. Teor. Fiz. **78**, 62 (1980) [Sov. Phys. JETP **51**, 31 (1980)].
[120]V. A. Bazylev and N. K. Zhevago, Phys. Status Solidi **b97**, 63 (1980).
[121]V. A. Bazylev and N. K. Zhevago, in: Eighth International Conference on Atomic Collisions in Solids, Abstracts, 1979, p. 91.
[122]V. A. Bazylev, V. I. Glebov, and N. K. Zhevago, in: Proceedings of the First National Conference on Radiation of Charged Relativistic Particles in Crystals, North Caucasus, USSR, May 22–25, 1980; Radiat. Eff. **56**, 99 (1981).
[123]a) A. L. Avakian, C. Yung, and N. K. Zhevago, Rad. Eff. **56**, 99 (1981); Zh. Eksp. Teor. Fiz. **82**, 584 (1982) [Sov. Phys. JETP **55**, 341 (1982)]; b) V. A. Bazylev and A. V. Demura, Radiat. Eff. **61**, 129 (1982).
[124]Y. Yamamura and Y. H. Ohtsuki, in a) Rad. Eff. **61**, 1 (1982); b) Phys. Rev. B **24**, 3430 [*sic*].

[125]K. Komaki and F. Fujimoto, Phys. Rev. B **24**, 13 [*sic*]; Phys. Lett. **A82**, 51 (1981).
[126]V. V. Beloshitskii and M. A. Kumakhov, Dokl. Akad. Nauk SSSR **235**, 331 (1980).
[127]V. A. Bazylev, V. V. Beloshitskiĭ, V. I. Glebov, N. K. Zhevago, M. A. Kumakhov, and Kh. Trikalinos, a) Dokl. Akad. Nauk SSSR **235**, 1100 (1977); b) Zh. Eksp. Teor. Fiz. **80**, 608 (1981) [Sov. Phys. JETP **53**, 306 (1981)]; Radiat. Eff. **56**, 87 (1981).
[128]R. W. Terhune and R. H. Pantell, Appl. Phys. Lett. **30**, 265 (1977).
[129]R. H. Pantell and M. J. Alguard, J. Appl. Phys. **34**, 798 (1979).
[130]A. I. Akhiezer, V. F. Boldyshev, and N. F. Shul'ga, Preprint KhFTI 77–38, Khar'kov Physicotechnical Institute, Khar'kov, 1977; Dokl. Akad. Nauk SSSR **236**, 830 (1977) [Sov. Phys. Dokl. **22**, 569 (1977)].
[131]A. I. Akhiezer, I. A. Akhiezer, and N. F. Shul'ga, Zh. Eksp. Teor. Fiz. **76**, 1244 (1979) [Sov. Phys. JETP **49**, 631 (1979)]; Preprint KhFTI 78–18, Khar'kov Physicotechnical Institute, Khar'kov, 1978.
[132]A. I. Akhiezer, V. F. Boldyshev, and N. F. Shul'ga, Fiz. Elem. Chastits At. Yadra. **10**, 51 (1979) [Sov. J. Part. Nucl. **10**, 19 (1979)].
[133]a) N. F. Shul'ga, Pis'ma Zh. Eksp. Teor. Fiz. **32**, 179 (1980) [JETP Lett. **32**, 166 (1980)]; b) N. F. Shul'ga, V. I. Truten', and S. P. Fomin, Preprint KhFTI 80–32, Khar'kov Physicotechnical Institute, Khar'kov, 1980.
[134]A. G. Bonch-Osmolovskiĭ and M. I. Podgoretskiĭ, Preprint R2-11250, Joint Institute for Nuclear Research, Dubna, 1978; Yad. Fiz. **29**, 432 (1979) [Sov. J. Nucl. Phys. **29**, 216 (1979)].
[135]V. N. Bayer, V. M. Katkov, and V. M. Strakhovenko, Phys. Lett. **A73**, 414 (1979).
[136]V. N. Baĭer, V. M. Katkov, and V. M. Strakhovenko, Dokl. Akad. Nauk SSSR **246**, 1347 (1979) [Sov. Phys. Dokl. **24**, 469 (1979)].
[137]V. N. Baĭer, V. M. Katkov, and V. M. Strakhovenko, Preprint IYaF-80-03, Institute of Nuclear Physics, Novosibirsk, 1980; Yad. Fiz. **33**, 1284 (1981) [Sov. J. Nucl. Phys. **33**, 686 (1981)].
[138]V. G. Baryshevskii and I. Ia Dubovskaya, Phys. Status Solidi **b82**, 403 (1977).
[139]V. G. Baryshevskii, A. O. Grubich, and I. Ia. Dubovskaia, Phys. Status Solid **83**, 351 (1978); **99**, 205 (1980).
[140]R. H. Pantell, Appl. Phys. Lett. **33**, 571 (1979).
[141]E. P. Eremeev and M. A. Kumakhov, Phys. Lett. **A72**, 359 (1979).
[142]N. A. Filatova, V. M. Golovatyuk, A. N. Iskakov, *et al*., Preprint Fermilab Pub.-81/34-EXP 7850.507-II, 1981.
[143]I. I. Miroshnichenko, D. D. Merri, R. O. Avakyan, and T. Kh. Figut, Pis'ma Zh. Eksp. Teor. Fiz. **29**, 786 (1979) [JETP Lett. **29**, 722 (1979)].
[144]A. O. Agan'yants, Yu. A. Vartanov, G. A. Vartapetyan, M. A. Kumakhov, Kh. Trikalinos, and V. Ya. Yaralov, Pis'ma Zh. Eksp. Teor. Fiz. **29**, 554 (1979) [JETP Lett. **29**, 505 (1979)].
[145]M. J. Alguard, R. L. Swent, and R. H. Pantell, Phys. Rev. Lett. **42**, 1148 (1979).
[146]R. L. Swent, R. H. Pantell, M. J. Alguard, B. L. Berman, S. D. Bloom, and S. Datz, Phys. Rev. Lett. **43**, 1723 (1979).
[147]R. H. Pantell and R. L. Swent, Appl. Phys. Lett. **35**, 910 (1979).
[148]S. A. Vorob'ev, V. I. Zabaev, V. N. Kalinin, V. V. Kaplin, and A. P. Potylitsyn, Pis'ma Zh. Eksp. Teor. Fiz. **29**, 414 (1979) [JETP Lett. **29**, 376 (1979)]; Yu. N. Adishchev, S. A. Vorob'ev, V. N. Eponeshnikov, V. V. Kaplin, and A. P. Potylitsyn, Pis'ma Zh. Tekh. Fiz. **5**, 1300 (1979) [Sov. Tech. Phys. Lett. **5**, 546 (1979)]; S. A. Vorob'ev, A. N. Didenko, V. N. Zabaev, B. N. Kalinin, V. V. Kaplin, A. A. Kurkov, A. P. Potylitsyn, and V. K. Tomchakov, Pis'ma Zh. Eksp. Teor. Fiz. **32**, 261 (1980) [JETP Lett. **32**, 241 (1980)].
[149]J. U. Andersen and E. Laegsgaard, Phys. Rev. Lett. **44**, 1079 (1980).
[150]N. Cue, E. Bonderup, B. B. Marsh, H. Bakhru, R. E. Benenson, R. Haight, K. Inglis, and G. O. Williams, Phys. Lett. **A80**, 26 (1980); Radiat. Eff. **56**, 9 (1981).
[151]V. B. Ganenko, L. É. Gendenshteĭn, I. I. Miroshnichenko, V. L. Morokhovskiĭ, E. V. Pegushin, V. M. Sanin, S. V. Shalatskiĭ, Pis'ma Zh. Eksp. Teor. Fiz. **32**, 397 (1980) [JETP Lett. **32**, 373 (1980)].
[152]R. Wedell, Phys. Status Solidi **b99**, **11** (1980).
[153]J. Lindhard, Phys. Lett. **12**, 126 (1964).
[154]C. Erginsoy, Phys. Rev. Lett. **15**, 360 (1965).
[155]G. Moliere, Z. Naturforsch **3a**, 78 (1948).
[156]B. R. Appleton, C. Erginsoy, and W. M. Gibson, Phys. Rev. **161**, 330 (1967).
[157]Yu. Kagan, Yu. V. Kononetz, and A. A. Mamontov, Phys. Lett. A72, 247 (1979).
[158]V. V. Kaplin and S. A. Vorob'ev, Fiz. Tverd. Tela (Leningrad) **19**, 1958 (1977) [Sov. Phys. Solid State **19**, 1145 (1977)].
[159]K. Komaki and F. Fujimoto, Phys. Lett. **A49**, 445 (1974).
[160]A. Tamura and T. Kawamura, Phys. Status Solidi **b73**, 391 (1976).
[161]P. Lervig, J. Lindhard, and V. Nielsen, Nucl. Phys. **A96**, 481 (1967).
[162]A. I. Akhiezer and V. B. Berestetskiĭ, Kvantovaya élektrodinamika (Quantum Electrodynamics), Nauka, Moscow, 1969 [Engl. Transl. of 2nd Ed. Interscience, 1965].
[163]B. Kagan and Yu. V. Kononets, Zh. Eksp. Teor. Fiz. **58**, 226 (1970) [Sov. Phys. JETP **31**, 124 (1970)]; **63**, 1041 (1973).
[164]V. A. Ryabov, Zh. Eksp. Teor. Fiz. **67**, 150 (1974) [Sov. Phys. JETP **40**, 77 (1975)].
[165]H. J. Kreiner, F. Bell, R. Sizmann, D. Harder, and W. Hüttl, Phys. Rev. **A33**, 135 (1970).
[166]E. M. Lifshitz and L. P. Pitaevskiĭ, Fizicheskaya kinetika (Physical Kinetics), Nauka, Moscow, 1979 [Engl. Transl. Pergamon Press, Oxford, 1981].
[167]V. V. Beloshitskiĭ and M. A. Kumakhov, Dokl. Akad. Nauk SSSR **212**, 846 (1973).
[168]M. A. Kumakhov, Usp. Fiz. Nauk **115**, 427 (1975) [Sov. Phys. Usp. **18**, 203 (1975)].
[169]V. V. Beloshitskiĭ and M. A. Kumakhov, Zh. Eksp. Teor. Fiz. **62**, 1144 (1972) [Sov. Phys. JETP **35**, 605 (1972)].
[170]A. Ia. Babudaev, V. V. Kaplin, and S. A. Vorobiev, Phys. Lett. **A45**, 71 (1973).
[171]A. Tamura and Y. H. Ohtsuki, Phys. Status Solidi **b62**, 447 (1974).
[172]F. Fujimoto and K. Komaki, in: International Crystal Conference Abstract of Papers, Melbourne, 1974, p. 274.
[173]F. Fujimoto, K. Komaki, H. Fujita, N. Sumita, Y. Uchida, K. Kambe, and G. Lehmphuhl, in: Atomic Collisions in Solids (ed. S. Datz, B. R. Appleton, and C. D. Moak), Plenum Press, New York, 1975, p. 547.
[174]V. V. Kaplin and S. A. Vorob'ev, Zh. Eksp. Teor. Fiz. **73**, 583 (1977) [Sov. Phys. JETP **46**, 304 (1977)]; Fiz. Tverd. Tela (Leningrad) **20**, 31 (1978) [Sov. Phys. Solid State **20**, 16 (1978)].
[175]V. V. Kaplin, D. E. Popov, and S. A. Vorobiev, Phys. Status Solidi **b76**, 779 (1976).
[176]A. Ya. Babudaev, S. A. Vorob'ev, V. V. Kaplin, S. V. Plotnikov, and D. E. Popov, Fiz. Tverd. Tela (Leningrad) **18**, 3131 (1976) [Sov. Phys. Solid State **18**, 1827 (1976)].
[177]A. Neufert, U. Shiebel, and G. Clausnitzer, Phys. Lett. **A26**, 49 (1975).
[178]U. Shiebel, A. Neufert, and G. Clausnitzer, Phys. Lett. **A42**, 45 (1972); **A47**, 13 (1974); Radiat. Eff. **29**, 57 (1976).
[179]H. Kumm, F. Bell, R. Sizmann, H. J. Kreiner, and D. Harder, Radiat. Eff. **12**, 53 (1972).
[180]F. Bell, H. J. Kreiner, and R. Sizmann, Phys. Lett. **A38**, 373 (1972).
[181]U. Schiebel and E. Worm, Phys. Lett. A58, 252 (1976).
[182]E. Uggerhøj, Phys. Lett. **A22**, 382 (1966).

[183]E. Uggerhøj and J. U. Andersen, Can. J. Phys. **46**, 543 (1968).
[184]R. Uggerhøj and F. Frandsen, Phys. Rev. **B2**, 582 (1970).
[185]J. U. Andersen, S. K. Andersen, and W. M. Augustyniak, Mat. Fiz. Dansk. Vid. Selsk. **38**, 101 (1977).
[186]S. K. Andersen, F. Bell, F. Frandsen, and E. Uggerhøj, Phys. Rev. **B8**, 413 (1973).
[187]D. E. Popov, V. V. Kaplin, and S. A. Vorobiev, Phys. Status Solidi **b96**, 263 (1979).
[188]J. U. Andersen, W. M. Augustyniak, and E. Uggerhøj, Phys. Rev. **B3**, 705 (1971).
[189]M. J. Pedersen, J. U. Andersen, and W. M. Augustyniak, Radiat. Eff. **12**, 47 (1972).
[190]I. A. Grishaev, G. V. Kovalenko, and B. I. Shramenko, Zh. Eksp. Teor. Fiz. **73**, 10 (1977) (*sic*).
[191]L. A. Gevorgyan and N. A. Korkhmazyan, Zh. Eksp. Teor. Fiz. **76**, 1226 (1979) [Sov. Phys. JETP **49**, 622 (1979)]; Phys. Lett. **A74**, 453 (1979).
[192]W. Gordon, Ann. d. Phys. **2**, 1031 (1929).
[193]L. D. Landau and E. M. Lifshitz, Kvantovaya mekhanika, Fizmatgiz, Moscow, 1963 (Quantum Mechanics: Non-Relativistic Theory, Addison-Wesley, Reading, Mass., 1965).
[194]K. Komaki and F. Fujimoto, Phys. Lett. A**82**, 51 (1981).
[195]M. J. Alguard, R. L. Swent, R. H. Pantell, S. Datz, J. H. Barrett, B. L. Berman, and S. D. Bloom, Nucl. Instrum. Meth. **170**, 7 (1980).
[196]a) N. P. Kalashnikov, É. A. Koptelov, and M. I. Ryazanov, Fiz. Tverd. Tela (Leningrad) **14**, 121 (1972); b) É. A. Koptelov and N. P. Kalashnikov, Preprint P-0054, Institute of Nuclear Research, Academy of Sciences of the USSR, Moscow, 1977.
[197]N. P. Kalashnikov and A. S. Ol'chak, in: Vzaimodeĭstviya yadernykh izlucheniĭ s monokristallami (Interaction of Nuclear Radiations with Single Crystals), MIFI, Moscow, 1979.
[198]N. P. Kalashnikov, V. S. Remizovich, M. I. Ryazanov, in: Stolknoveniya bystrykh zaryazhennykh chastits v tverdykh telakh (Collisions of Fast Charged Particles in Solids), Atomizdat, Moscow, 1980.
[199]a) V. L. Ginzburg and V. Ya. Éĭdman, Zh. Eksp. Teor. Fiz. **36**, 1823 (1959) [Sov. Phys. JETP **9**, 1300 (1959)]; b) V. L. Ginzburg, Izv. Akad. Nauk SSSR, Ser. Fiz. **11**, 165 (1947).
[200]H. Motz, J. Appl. Phys. **22**, 527 (1951).
[201]N. A. Korkhmazyan, Izd. Akad. Arm. SSR Ser. Fizika **5**, 287 (1970); **7**, 113 (1972).
[202]D. F. Alferov, Yu. A. Bashmakov, and E. G. Bessonov, a) Zh. Tekh. Fiz. **42**, 1929 (1972) [*sic*]; b) **43**, 2126 (1973) [Sov. Phys. Tech. Phys. **18**, 1336 (1973)]; c) Tr. FIAN SSSR **80**, 100 (1975).
[203]V. N. Baĭer, V. M. Katkov, and V. M. Strakhovenko, Zh. Eksp. Teor. Fiz. **63**, 2121 (1972) [Sov. Phys. JETP **36**, 120 (1973)].
[204]Yu. G. Pavlenko, V. I. Petukhov, and A. Kh. Mussa, Izv. Akad. Nauk SSSR, Ser. Fiz. **10**, 88 (1973).
[205]V. G. Bagrov, D. M. Gitman, A. A. Sokolov, I. M. Ternov, N. I. Fedosov, and V. R. Khalilov, Zh. Tekh. Fiz. **45**, 1948 (1975) [Sov. Phys. Tech. Phys. **20**, 1226 (1975)].
[206]A. A. Sokolov, D. V. Gal'tsov, and V. U. Zhukovskiĭ, Zh. Tekh. Fiz. **43**, 682 (1973) [Sov. Phys. Tech. Phys. **18**, 430 (1973)].
[207]I. I. Gol'dman, Zh. Eksp. Teor. Fiz. **46**, 1412 (1964) [Sov. Phys. JETP **19**, 954 (1964)]; Phys. Lett. **8**, 103 (1964).
[208]V. M. Galitskiĭ and V. P. Yakovlev, Preprint, Institute of Nuclear Physics, Siberian Branch, Academy of Sciences of the USSR, Novosibirsk, 1964.
[209]A. I. Nikishov and V. I. Ritus, Zh. Eksp. Teor. Fiz. **46**, 776 (1964) [Sov. Phys. JETP **19**, 529 (1964)]; Tr. FIAN SSSR **111**, 3 (1979).
[210]V. N. Baĭer, V. M. Katkov, and V. M. Strakhovenko, Zh. Eksp. Teor. Fiz. **80**, 1348 (1981) [Sov. Phys. JETP **53**, 688 (1981)].
[211]M. Gouanere, D. Sillou, M. Spighel, N. Cue, M. J. Gaillard, R. G. Kirsch, J. C. Poizat, J. Remilleux, B. L. Berman, P. Catillon, L. Roussel, and G. M. Temmer, Preprint LAPP-EXP-05, 1981.
[212]V. A. Bazylev and V. V. Goloviznin, Zh. Eksp. Teor. Fiz. **82**, 1204 (1982) [Sov. Phys. JETP **55**, 800 (1982)]; Radiat. Eff. **60**, 101 (1982).
[213]V. V. Beloshitskiĭ and M. A. Kumakhov, Dokl. Akad. Nauk SSSR, **259**, 341 (1981) [Sov. Phys. Dokl. **27**, 682 (1981)]; V. V. Beloshitskiĭ and Kh. Trikalinos, in: Predvaritel'naya programma i tezisy X Vsesoyuznogo soveshchaniya po vzaimodeĭstviyu puchkov zaryazhennykh chastits s tverdym telom (Preliminary Program and Abstracts, Tenth All-Union Conference on the Interaction of Charged-Particle Beams with Solids), Izd. Mosk. Univ., Moscow, 1979, p. 35.
[214]J. E. Watson and J. S. Koehler, Phys. Rev. **A24**, 861 (1981).
[215]K. Komaki and F. Fujimoto, Radiat. Eff. **56**, 13 (1981).

Translated by Dave Parsons